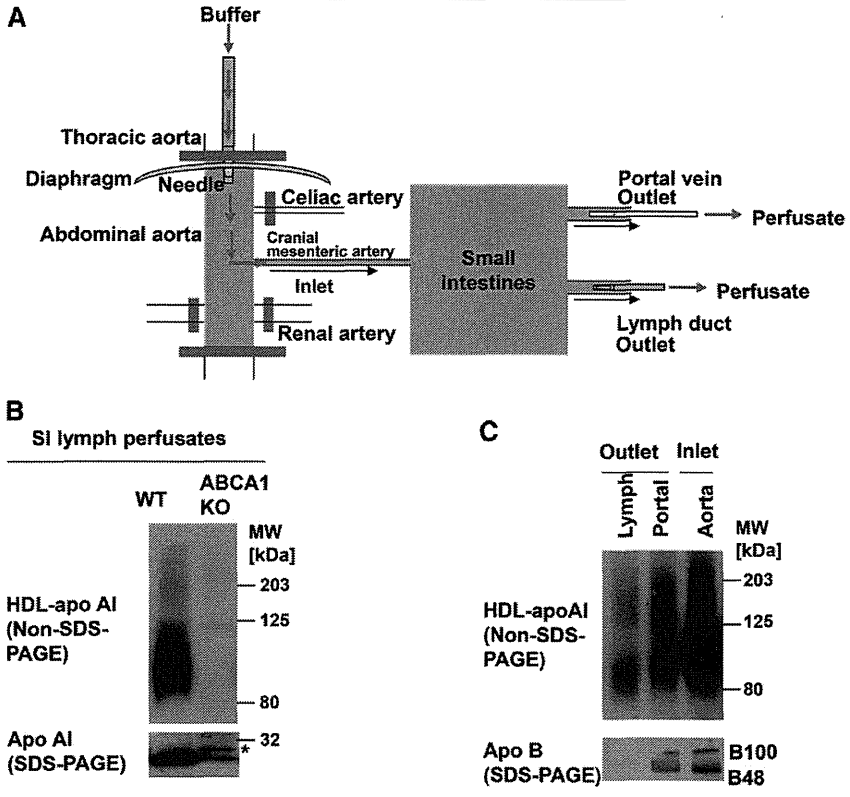

Fig. 1. Establishment of an in situ perfusion model of mouse SI and analyses of lipoproteins in the SI lymph perfusates. A: A schematic representation of our in situ perfusion system for assessing HDL production in mouse SI. The abdominal aorta and its branches were ligated as shown in red bars, and the aorta was punctured and cannulated to serve as the inlet (supplementary Fig. I). The portal vein and intestinal lymph duct were punctured and cannulated to serve as outlets. Flow of the perfusion buffer was shown by the arrows. The mouse body and perfusion buffer were warmed to 35°C before perfusion was started. B: Non-SDS-PAGE analysis of HDL-apo AI (upper panel) and SDS-PAGE analysis of apo AI (lower panel) in SI lymph perfusates from WT (left lane) and ABCA1 KO (right lane) mice. C: Non-SDS-PAGE analysis of HDL-apo AI (upper panel) and SDS-PAGE analysis of apo B48 and apo B100 (lower panel) in perfusates from the SI lymph duct and portal vein of ABCA1 KO mice perfused with buffer containing serum from WT mice.

non-SDS-PAGE, transferred to polyvinylidene difluoride membranes, and immunoblotted with anti-mouse apo AI, apo AIV, apo E, apo B100, or apo B48 overnight at 4°C. Membranes were washed and then incubated with anti-IgG antibody conjugated with HRP for 1 h at room temperature. An ECL Advance Western Blotting Detection Kit (Amersham Biosciences, Piscataway, NJ) was used for the visualization of immunoblots according to the manufacturer's protocol.

Conventional SI lymph cannulation experiments

After intraperitoneal anesthesia, the main mesenteric lymphatic duct of WT mice was cannulated as previously described by Green et al. (14). HDL was separated by ultracentrifugation from a sample of mesenteric lymph and used for the analysis of HDL proteins using LC/MS.

In situ perfusion system for the evaluation of HDL production in the liver

In situ perfusion for the liver from WT mice was performed according to the method reported by Sugano et al. (28) with minor modifications. Briefly, after the mice were deeply anesthetized, the abdomen was opened, the portal vein was cannulated in situ, and the liver was perfused with oxygenated buffer, which was the same as that used for in situ perfusion of the SI. To prevent swelling of the liver, the abdominal vena cava was incised immediately after cannulation, the thorax was opened, a part of the inferior vena cava was cut, and a cannula was inserted.

After the collected perfusate was concentrated using centrifugal filter devices (Millipore), HDL was separated by ultracentrifugation and used for the analysis of HDL proteins using LC/MS, analysis of the HDL lipid composition using HPLC, and analysis of the HDL apo composition.

MS analysis of HDL fractions

HDL fractions from mouse serum, SI lymph perfusate, SI lymph (14), and liver perfusate (28) from WT mice were buffer exchanged with 10 mM triethylammonium bicarbonate buffer (Sigma-Aldrich, St. Louis, MO) and concentrated by centrifugation (6,000 *g*, 30 min at 4°C) using Vivaspin2 (MW 3000; GE Healthcare, Buckinghamshire, UK). The protein concentration of each sample was determined with the Bradford method and adjusted to 7.5 mg/ml. Ten microliters of each sample was then subjected to reduction and alkylation [1 μl of denaturant and 2 μl of reducing reagent (AB Sciex, Foster City, CA)] for 60 min at 60°C, cystein blocking [1 μl of cystein-blocking reagent (AB Sciex)], and trypsinization [1.9 μg of trypsin (Roche, Basel, Switzerland)] for 4 h at 37°C followed by the addition of another 1.9 μg of trypsin and overnight incubation at 37°C. After digestion,

ASBMB JOURNAL OF LIPID RESEARCH

the samples were desalted and concentrated with C18 Stage tips (29) packed in-house in 60 μl of 2% acetonitrile (ACN) and 0.1% trifluoroacetic acid (TFA) buffer.

Each sample was fractionated for 70 min by HPLC (Prominence; Shimazu, Kyoto, Japan) using an SCX column [ZORBAX 5 μm 300-SCX 2.1 × 50 mm (Agilent Technologies, San Jose, CA)] at a flow rate of 10 μl/min with a KCl gradient of from 0 to 1 M in 10 mM KH_2PO_4/25% ACN solution, as described previously (30). The fractionated peptides (36 fractions) were lyophilized to dryness, and the dried peptides were reconstituted in 20 μl of 0.1% formic acid in 2% ACN and analyzed with a QSTAR Elite mass spectrometer (AB Sciex) coupled online to a nanoflow HPLC (Paradigm MS2; Michrom Bioresources, Auburn, CA) with an autosampler (HTS-PAL; CTC Analytics AG, Zwingen, Switzerland) using a nanospray ionization source (NanoSprayII; AB Sciex) that held 3 μm inner-diameter C18 columns (L-column2 ODS; Chemicals Evaluation and Research Institute, Tokyo, Japan) packed in-house into 20 cm long, 75 μm inner-diameter fused silica emitters pulled on a P-2000 Laser Based Micropipette puller (Sutter Instruments, Novato, CA). The samples were run at a flow rate of 200 nl/min with an ACN gradient (0–85 min, ACN 2%–33%; 85–95 min, ACN 33%–86%) in 0.1% formic acid.

Lipid profile analyses using HPLC

Two hundred microliters of SI lymph perfusates or HDL separated by ultracentrifugation from plasma, SI lymph perfusates, and liver perfusates from WT mice was analyzed with the HPLC system using two tandem gel permeation columns (Lipopropak XL, 7.8 mm × 300 mm; Tosoh Corp., Tokyo, Japan) at a flow rate of 700 μl/min. Total cholesterol (TC), TG, free cholesterol (FC), and phospholipid (PL) were measured with two parallel online enzymatic lipid detection systems (350 μl/min each) (Skylight Biotech, Inc., Akita, Japan) (31–34). The system was calibrated with the aid of latex beads and high-molecular-weight standards for the apparent spherical diameters of HDL.

Isolation of lipoproteins by ultracentrifugation

Lipoprotein fractions were isolated from SI lymph perfusates, SI lymph, liver perfusates, and plasma from WT mice by serial preparative ultracentrifugation as described previously (35–39). Briefly, SI lymph perfusate was overlaid with saline solution at a volume ratio of ~5:3 and ultracentrifuged at 50,000 *g* for 25 min (2.25×10^6 g/min) (40) at 10°C in a TLA-100.2 rotor in a Beckman TL-100 Tabletop Ultracentrifuge (Beckman Instruments Inc.). Chylomicron (CM) fraction (upper fraction) was collected using a tube slicer. The bottom fraction was overlaid with saline and ultracentrifuged at 100,000 rpm for 2 h at 10°C. The VLDL fraction (upper fraction) was collected using a tube slicer. The density of the d > 1.006 g/ml fraction (bottom fraction) was then adjusted to 1.063 g/ml with solid KBr and overlaid with d = 1.063 g/ml KBr solution. After centrifugation at 100,000 rpm for 2 h at 10°C, the LDL fraction (upper fraction) was collected. Finally, the density of the d >1.063 g/ml fraction (bottom fraction) was adjusted to 1.25 g/ml with solid KBr and overlaid with d = 1.25 g/ml KBr solution. After centrifugation at 100,000 rpm for 5 h at 10°C, the HDL fraction (upper fraction) was collected with a tube slicer. LDL and HDL fractions were dialyzed against saline containing EDTA (1 mM) to eliminate KBr. HDL for lipid profile analyses using HPLC and determination of protein concentration was used without dialysis.

Electron microscopy of HDL particles

The size distributions of HDL particles separated from SI lymph perfusates and plasma of WT mice were examined by electron microscopy (EM), as described previously (35). In brief, for transmission electron microscopy (TEM), HDL was separated by preparative ultracentrifugation and dialyzed against saline containing 1 mM EDTA (pH 8.0) overnight at 4°C to remove KBr. Next, HDL was dialyzed against a 10 mM NH_4HCO_3 solution for 2 h at 4°C and negatively stained with 1% uranium acetate. Electron micrographs were obtained with a computer-controlled JEOL 1200EX electron microscope (JEOL Inc., Tokyo, Japan). Images at a final magnification of 200,000× were acquired with a high-resolution digital camera. The diameters of spherical HDL particles were measured using TEM imaging Platform iTEM (Olympus Soft Imaging Solutions GmbH, Münster, Germany).

Two-dimensional gel electrophoresis

To examine the effects of LCAT inhibition on SI-HDL production, HDL in SI lymph perfusates collected using the in situ perfusion technique from WT mice with and without the presence of DTNB in the perfusion buffer was separated by native two-dimensional gel electrophoresis as described previously (41, 42). Fresh SI lymph perfusates were run on an agarose gel (0.75%) and then on a 2% to 25% polyacrylamide gel at 0°C at 100 V for 20 h. Fractionated HDL was electroblotted to a nitrocellulose sheet at 0°C and detected with the following antibodies. The first antibody was a rabbit anti-mouse apo AI antibody (BioDesign), and the second was a goat anti-rabbit IgG (DAKO) iodinated with $Na^{125}I$ by a modified chloramine T method.

Statistical data analysis

Statistical data analyses were performed using the Statistical Analysis System (SAS) Software Package (Ver. 9.2; SAS Institute Inc., Cary, NC) at Fukuoka University (Fukuoka, Japan). Differences in the lipid and protein composition of HDL between groups were examined by an ANOVA using the general linear model (43). Differences in the size of HDL particles between plasma HDL and SI-HDL were examined by the Wilcoxon rank sum test. Data are presented as the mean ± SD, and the significance level was considered to be <0.05 unless indicated otherwise.

RESULTS

Development of a novel in situ perfusion model in mice

A novel in situ perfusion model was developed in mice with isolated SI in which the arterial blood supply for the SI is blocked, leaving only the superior mesenteric artery open as the perfusion inlet for the SI. Fig. 1A shows a schematic representation of our novel in situ perfusion model. Because the source of HDL obtained from the mesenteric lymph duct of anesthetized rodents in vivo is either the secretion of HDL by SI or the filtration of HDL from plasma through the blood capillary-lymph loop into the intestinal lymph duct (19–22), in our in situ perfusion model the arterial blood supply for the SI was blocked by ligation of the abdominal aorta and its branches (Fig. 1A) to dissociate the HDL produced by the SI from HDL filtered from plasma.

The superior mesenteric artery was not ligated and was left open as the perfusion inlet (Fig. 1A). A 26G needle was inserted antegrade from the thoracic descending aorta into the abdominal aorta before ligation of the abdominal aorta and used to pump perfusion buffer through the

abdominal aorta into the mesenteric artery (Fig. 1A). The portal vein and intestinal lymph duct were punctured and cannulated to serve as outlets (Fig. 1A). Therefore, in our in situ perfusion mouse model, no further systemic blood will come into the SI after perfusion with a buffer solution starts, and thus the HDL in the infusates collected from the SI lymph duct (one of the outlets) would only be produced from the SI and not infiltrate from the systemic plasma.

The SI produces HDL

The intestine and liver are the two major sites of HDL production (15, 16, 44). To demonstrate that the SI produces HDL, SI lymph perfusates were collected from WT mice using our in situ perfusion model. Nondenaturing PAGE followed by Western blot analysis for apo AI, the major protein of HDL, clearly showed that HDL from the SI was present in SI lymph perfusate (Fig. 1B, left lane of the upper panel), but not in perfusate collected from the portal vein (data not shown). Because systemic blood does not come into the SI during perfusion due to the blockade of systemic blood by ligation of the abdominal aorta and its branches in our in situ perfusion model, this result indicates that the SI produces HDL in WT mice.

ABCA1 is required for the production of HDL from the SI

Intestinal ABCA1 has been shown to contribute to HDL biogenesis in mice in vivo (16). To clarify the influence of ABCA1 on the production of HDL from the SI, we collected lymph perfusates from ABCA1 KO mice using our in situ perfusion model. HDL-apo AI was not detected in SI lymph perfusates from ABCA1 KO mice (Fig. 1B, right lane of the upper panel). This result indicates that ABCA1 is required for the production of HDL from the SI.

However, an apo AI immunoreactive mass was detected in the form of doublets in the SI lymph perfusate from ABCA1 KO mice, in contrast to a major single band that was detected in that from WT mice (Fig. 1B, lower panel). It is possible that the upper band in ABCA1 KO mice may represent a precursor of apo AI, newly synthesized from the intestine. Therefore, the deficient HDL production from the SI of ABCA1 KO mice was not due to the defective synthesis of apo AI, but rather to the defective lipidation of apo AI (45).

Evidence that plasma HDL can filtrate from the abdominal aorta into the SI lymph duct

Although a previous study suggested that plasma HDL can infiltrate into the mesenteric lymph (16), there is still some controversy, and direct evidence is not available. We used our in situ perfusion model to clarify whether plasma lipoproteins in abdominal aorta contribute to HDL in SI lymph. Because ABCA1 KO mice showed the deficient production of HDL from the SI (Fig. 1B), the addition of serum from WT mice to the perfusion buffer should be able to show whether plasma HDL can infiltrate from the abdominal aorta to the mesenteric lymph duct.

Therefore, we used ABCA1 KO mouse bodies for in situ perfusion but added serum from WT mice to the perfusion buffer. Perfusates from the abdominal aorta (inlet) and lymph duct and portal vein (two outlets) were run on nondenaturing PAGE followed by Western blot analysis for apo AI and on SDS-PAGE followed by Western blot analysis for apo B100 and apo B48 (Fig. 1C). As shown in the upper panel of Fig. 1C, a substantial amount of HDL was present in the perfusates collected from both the SI lymph duct and the portal vein. Because SI-HDL is not formed in ABCA1 KO mice due to the defect in the lipidation of apo AI, HDL detected in SI lymph perfusates should come from the infiltration of plasma HDL from the abdominal aorta.

Apo B was detected in perfusates collected from the portal vein, but not in SI lymph perfusates (Fig. 1C, lower panel). Because no apo B was detected in SI lymph perfusates, our result indicates that apo-B-containing lipoprotein was not filtrated from the abdominal aorta into the lymph duct.

Mapping of peptides from intestinal HDL and hepatic HDL using LC/MS

A previous study has shown that HDL from the intestinal lymph duct obtained in vivo from anesthetized mice is likely to contain HDL from the systemic circulation, most of which was derived from the liver (16). Therefore, we compared the SI-HDL obtained using our novel in situ perfusion mouse model, the intestinal HDL (C-HDL) obtained in vivo from anesthetized mice using a conventional experimental procedure, and hepatic HDL (L-HDL) obtained from liver perfusion. Protein moieties of HDL from mouse plasma (P-HDL), SI-HDL, C-HDL, and L-HDL were compared by using LC/MS (**Fig. 2**).

As shown in Fig. 2, the peptide patterns of C-HDL were very similar to those of L-HDL: the same number of major peptides was detected (m/z 543, 402, 403, 523, 413, 422, and 435), and they had similar relative peptide-ion intensities. These results suggest that C-HDL may contain HDL from the systemic circulation, most of which is derived from the liver (16).

However, the peptide patterns of SI-HDL were apparently different from those of C-HDL and L-HDL: SI-HDL had additional peptides of m/z 542 and 524 that were not detected in C-HDL and L-HDL (Fig. 2B, indicated by red arrows). Because HDL obtained using our novel in situ perfusion technique is not subject to interference from the liver and plasma, our results indicate that intestinal HDL is different from hepatic HDL and that the novel in situ perfusion model is suitable for the selective evaluation for SI-HDL.

Distribution of lipids and apos in lipoproteins produced from the SI

To characterize lipoproteins produced from the SI, we examined the distribution of lipids and apos in lymph perfusates collected from WT mice using our novel in situ perfusion model. Lipid profiles were analyzed by online monitoring for TC, FC, TG, and PL after lipoproteins

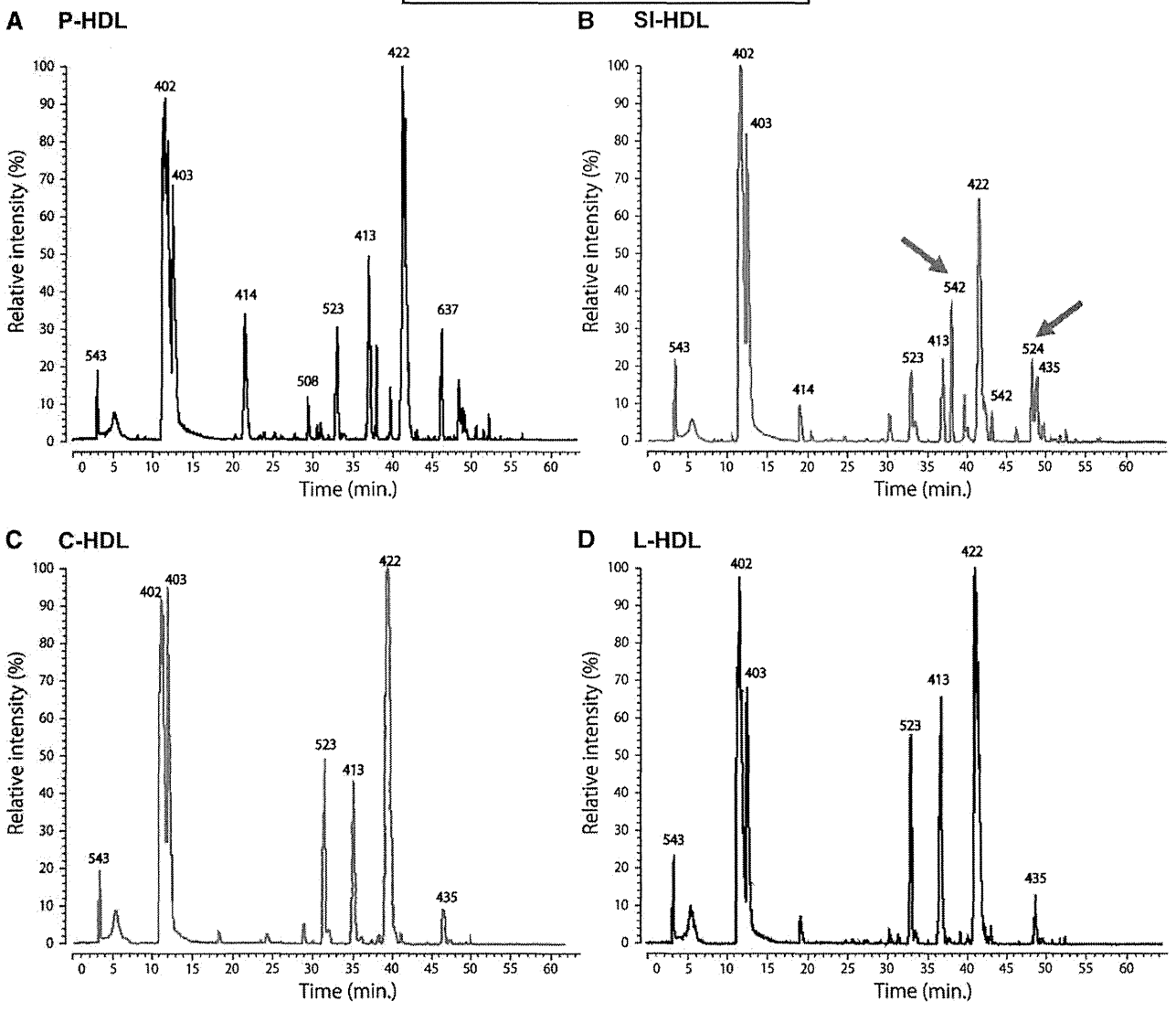

Fig. 2. Comparison of plasma HDL, intestinal HDL, and hepatic HDL in WT mice by peptide mapping using LC/MS. A–D: LC/MS total ion chromatograms of peptides, in which peptide-ion intensity is shown as a function of the peptide retention time, for HDL separated by ultracentrifugation from plasma (P-HDL) (A), SI lymph perfusates (SI-HDL) obtained using a novel in situ perfusion model (B), mesenteric lymph (C-HDL) obtained by conventional intestinal lymph cannulation experiments (C), and liver perfusates (L-HDL) (D) of WT mice. The numerical value of each peak shows *m/z* of representative peptides included in the peak. Arrows indicate peptides with *m/z* 542 and 524 detected specifically in SI-HDL.

were separated by HPLC (**Fig. 3A**). As shown in Fig. 3A, lipoproteins in SI lymph perfusates were separated into two main fractions, one corresponding to plasma HDL and another corresponding to plasma non-HDL (CM to VLDL size). The four main classes of lipids (i.e., cholesterol ester [CE], FC, TG, and PL) were mainly distributed in the non-HDL fraction (Fig. 3A), similar to plasma lipoproteins.

To examine the distribution of apos, lipoprotein density fractions (CM, VLDL, LDL, and HDL) were separated from lymph perfusates of WT mice by small-scale preparative ultracentrifugation. Apo AI, apo AIV, apo B100, and apo B48 in each lipoprotein density fraction were detected by Western blot analysis after separation by SDS-PAGE (Fig. 3B). As shown in Fig. 3B, lipoproteins produced from the SI contained only apo B48, and no apo B100, as expected (46). Apos were not detected in the LDL fraction separated from lymph perfusates (Fig. 3B), indicating that the LDL-size fraction was not produced by the SI. HDL from SI lymph perfusates contained both apo AI and AIV, similar to plasma HDL (Fig. 3B).

Lipid and protein composition of SI-HDL

WT mice were used to examine the lipid and protein composition of HDL produced from the SI. HDL was separated from plasma, SI lymph perfusates collected using our in situ perfusion model, and liver perfusates using small-scale preparative ultracentrifugation. HDL separated by ultracentrifugation was used for the measurement of total protein and apos but was further separated using HPLC for the online

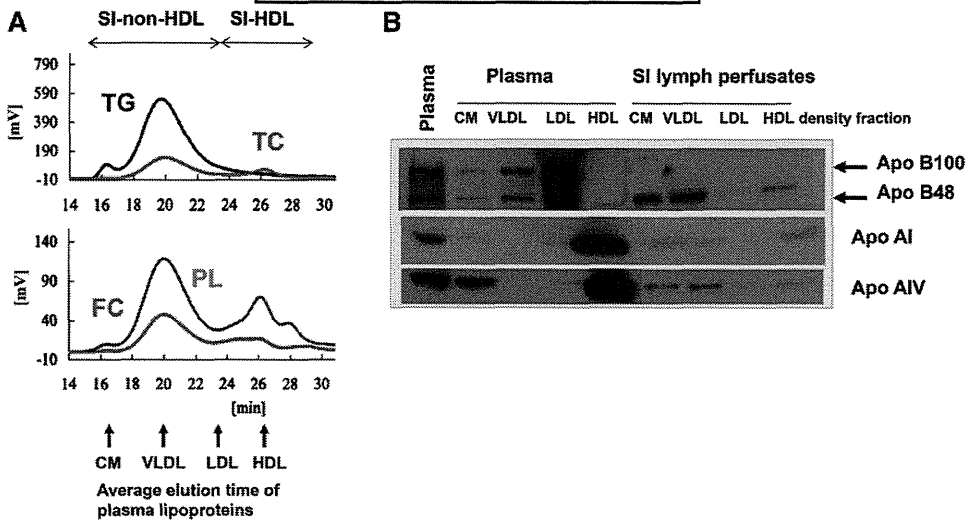

Fig. 3. HPLC analyses of lipids and preparative ultracentrifugation followed by Western blotting for apos in SI lymph perfusates. A: HPLC analyses of SI lymph perfusates from WT mice. Two hundred microliters of SI lymph perfusates was run on HPLC as described in the Methods. TC, FC, TG, and PL were measured enzymatically. Arrows denote the average elution time of indicated plasma lipoproteins in WT mice. B: Apo distribution among lipoproteins in SI lymph perfusates from WT mice separated by preparative ultracentrifugation. Lipoproteins in plasma and SI lymph perfusates were subjected to small-scale preparative ultracentrifugation to concentrate samples, and the concentrated samples were then run on SDS-PAGE followed by Western blot analysis using antibodies against the indicated apos. CM, VLDL, LDL, and HDL denote the density range of the indicated plasma lipoprotein fractions.

measurement of lipids to ensure that lipids in HDL are measured without possible interference from other lipoproteins. Supplementary Fig. II gives examples of the HPLC TC profile of HDL separated from plasma, lymph perfusates, and liver perfusates to show the purity of HDL. HPLC-separated HDL was measured for TC, TG, FC, and PL, and CE was calculated from TC and FC (47).

Table 1 and **Fig. 4A** show the contents of lipids and total protein in P-HDL, L-HDL, and SI-HDL. SI-HDL, similar to L-HDL, had a significantly higher protein content and lower lipid content than P-HDL (Table 1, Fig. 4A). CE and PL were the major lipids in SI-HDL and L-HDL, similar to P-HDL. However, the contents of CE and PL relative to protein in SI-HDL and L-HDL were significantly lower than those in P-LDL (Table 1).

Table 1 also shows the distribution of lipids in HDL. At ad libitum, SI-HDL tended to show less CE and more TG than P-HDL and L-HDL (Table 1). The distribution of CE and TG was significantly ($P < 0.05$) different between SI-HDL and L-HDL at ad libitum and between SI-HDL at ad libitum and at fasting, as assessed by a two-way ANOVA (data not shown). At fasting, TG was not detected in L-HDL but was detected in SI-HDL (Table 1).

Therefore, using our in situ perfusion model, we showed that SI-HDL was protein rich compared with HDL in plasma in WT mice and TG rich compared with L-HDL.

TABLE 1. Lipid and protein composition of HDL separated by ultracentrifugation from mouse plasma, liver perfusates, and SI lymph perfusates collected using an in situ perfusion model

	HDL in Plasma	HDL Produced from the Liver		HDL Produced from the SI	
	Ad libitum (n = 5)	Ad libitum (n = 5)	Fasting (n = 5)	Ad libitum (n = 5)	Fasting (n = 5)
HDL composition (% total mass)					
Protein	55.3 ± 2.1	83.8 ± 9.0[a]	83.3 ± 6.5[a]	86.0 ± 5.0[a]	88.8 ± 4.4[a]
Lipids	44.7 ± 2.1	16.2 ± 9.0[a]	16.7 ± 6.5[a]	14.0 ± 5.0[a]	11.2 ± 4.4[a]
FC	2.2 ± 0.5	1.0 ± 0.6[a]	1.3 ± 0.2[b]	1.3 ± 1.1	0.9 ± 0.7[a]
CE	17.9 ± 0.4	5.9 ± 2.9[a]	6.7 ± 2.9[a]	3.7 ± 2.2[a]	4.1 ± 1.8[a]
PL	24.1 ± 2.1	9.1 ± 5.5[a]	8.7 ± 3.7[a]	6.8 ± 2.2[a]	5.8 ± 3.6[a]
TG	0.5 ± 0.3	0.2 ± 0.4	0.0 ± 0.0[a]	2.3 ± 2.9	0.4 ± 0.9
HDL lipid composition (% of lipid mass)					
FC	5.0 ± 1.2	6.6 ± 6.1	8.5 ± 3.7	11.2 ± 13.4	7.0 ± 5.5
CE	40.1 ± 2.1	38.7 ± 9.8	39.3 ± 4.1	24.2 ± 14.0[a, c]	41.0 ± 18.4
PL	53.8 ± 2.3	54.2 ± 6.2	52.2 ± 2.5	50.2 ± 14.1	49.2 ± 17.9
TG	1.1 ± 0.6	0.6 ± 1.3	0.0 ± 0.0	14.3 ± 14.9[b, c]	2.8 ± 6.2

[a] $P < 0.05$, versus plasma, assessed by an ANOVA.
[b] $P < 0.1$, versus plasma, assessed by an ANOVA.
[c] $P < 0.1$, versus the liver, assessed by an ANOVA.

ASBMB JOURNAL OF LIPID RESEARCH

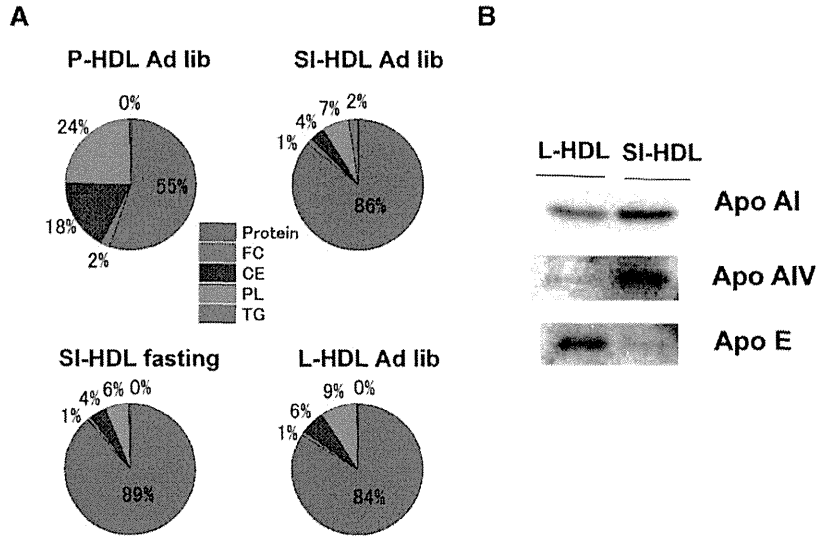

Fig. 4. Lipid and apo composition of HDL in SI lymph perfusates from WT mice. A: Lipid and protein composition of HDL in plasma (P-HDL), SI lymph perfusates (SI-HDL), and liver perfusates (L-HDL) separated by serial preparative ultracentrifugation. HDL was further separated by HPLC to determine its lipid composition. B: Comparison of apo compositions of SI-HDL and L-HDL. SI-HDL and L-HDL were obtained by in situ perfusion followed by serial preparative ultracentrifugation and subjected to SDS-PAGE followed by Western blot analysis using antibodies against the indicated apos.

Apo composition of SI-HDL

To characterize the apo composition of SI-HDL, L-HDL and SI-HDL separated by ultracentrifugation from liver perfusates and SI lymph perfusates, respectively, were run on SDS-PAGE and then subjected to Western blot analysis for apo AI, apo AIV, and apo E (Fig. 4B). As shown in Fig. 4B, L-HDL contained a very limited amount of apo AIV but a considerable amount of apo E, whereas an opposite trend was seen for SI-HDL. This result indicates that SI-HDL was rich in apo AIV compared with L-HDL, and SI-HDL is different from L-HDL with respect to the composition of apos.

Size distribution of SI-HDL

Because SI-HDL was protein rich compared with P-HDL (Table 1), we used EM to examine the size distribution of HDL separated using ultracentrifugation from SI lymph perfusates and plasma of WT mice (**Fig. 5**). Fig. 5A shows the representative negative-stain electron micrographs of SI-HDL and P-HDL. As shown, SI-HDL particles were a population of spheres with a very small number of discs. We measured the particle diameter of spherical particles in SI-HDL and P-HDL (Fig. 5B, C). Fig. 5B shows the size distribution of SI-HDL and P-HDL. As shown, SI-HDL particles, similar to P-HDL, were heterogeneous in size, but the distribution of SI-HDL particles was more diverse than that of P-HDL, and the size distributions of SI-HDL and P-HDL overlaid (Fig. 5B). However, SI-HDL apparently had a higher proportion of smaller particles as compared with P-HDL (Fig. 5B). Fig. 5C shows the individual data and the box plots of SI-HDL and P-HDL. As shown, although the size range of SI-HDL covered that of P-HDL, the peak diameter of SI-HDL particles shifted toward smaller particles as compared with that of P-HDL, and the average size of SI-HDL particles (mean ± SD: 11.06 ± 2.70 nm) was significantly ($P < 0.001$) smaller than that of P-HDL particles (12.94 ± 1.64 nm). This result indicates that the particle size of SI-HDL was smaller than that of P-HDL.

Inhibitors of ABCA1 and LCAT affect the formation of SI-HDL

Because we have shown that most of the HDL particles secreted from the SI are spherical using EM (Fig. 5A), to identify the mechanism for SI-HDL assembly, we examined the effects of inhibitors of ABCA1 and LCAT on the formation of SI-HDL. It is well known that ABCA1 lipidates apo AI to form HDL and LCAT converts lipid-poor pre-β-migrating HDL to mature α-migrating HDL. We used glyburide (26) and DTNB (27) as inhibitors of ABCA1 and LCAT, respectively (**Fig. 6A**). The effects of ABCA1 and LCAT inhibitors were examined by collecting SI lymph perfusates from WT mice that underwent in situ perfusion using buffers with and without the presence of the inhibitors (Fig. 6).

As shown in Fig. 6B, nondenaturing PAGE followed by Western blot analysis for apo AI showed that there was a marked increase in free apo AI and small HDL in SI lymph perfusates in the presence of glyburide compared with the absence of glyburide. This result suggests that ABCA1 is involved in the lipidation of apo AI to form SI-HDL.

As shown in Fig. 6C, two-dimensional electrophoresis of SI lymph perfusates followed by Western blotting for apo AI showed that the presence of premature HDL such as pre-β1- and pre-β2-HDL (41, 42) was observed in the presence of DTNB, but not in the absence of DTNB. A reduction in α-HDL particle size was also observed in the

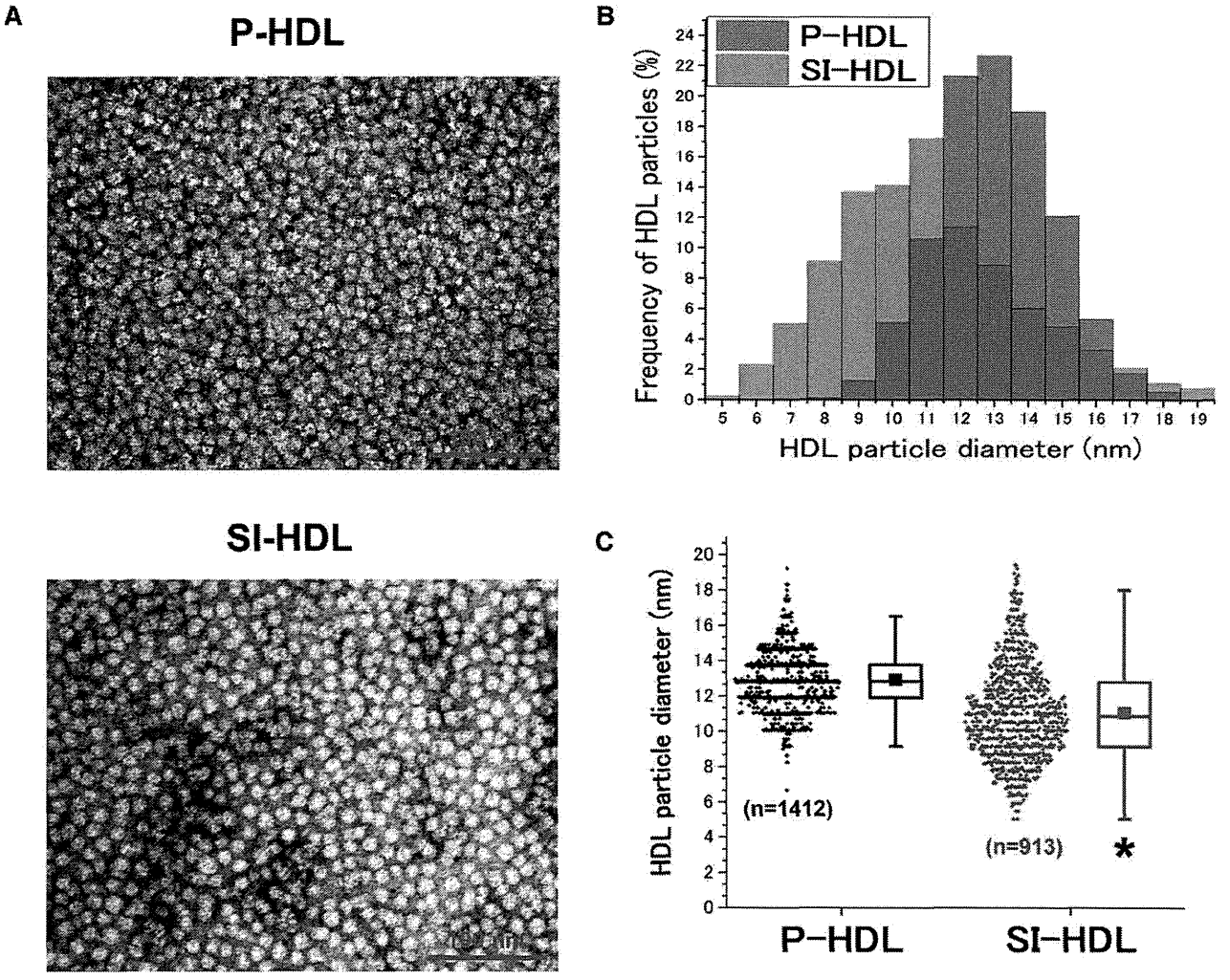

Fig. 5. Electron micrographs of negatively stained HDL from SI lymph perfusates. A: Representative negative-stain EM of HDL separated by serial ultracentrifugation from SI lymph perfusates (SI-HDL, lower panel) and plasma (P-HDL, upper panel). Magnification: 200,000×; scale bar: 100 nm. B: Size distribution of SI-HDL and P-HDL particles from negative-stain electron micrographs. The frequency distributions of the size of SI-HDL (pink bars; n = 913) and P-HDL (gray bars; n = 1,412) were plotted together, and the red bars represent the overlaid parts. Two measurements were made for the diameter of each HDL particle, and the mean diameter was used to calculate the size frequency. C: Box-and-whisker plots showing the mean (■), median (middle bar in the rectangle), and 10th (bottom bar), 25th (bottom of rectangle), 75th (top of rectangle), and 90th (top bar) percentiles of the sizes of SI-HDL (black) and P-HDL (red) particles. The individual data are shown on the left of the boxes. * $P < 0.001$, SI-HDL versus P-HDL, assessed by the Wilcoxon rank sum test.

presence of DTNB (Fig. 6C). This result suggests that LCAT may be involved in the maturation of SI-HDL.

Although our experiments were limited in that the inhibitory effects of ABCA1 and LCAT are unknown, our results suggest that ABCA1 and LCAT may play important parts in the formation of SI-HDL.

Nutritional regulation of the production of HDL from SI

A previous study showed that intestine significantly contributes to plasma HDL-C levels (44). We examined the effects of fasting and high-fat feeding on the production of HDL from SI in WT mice using our in situ perfusion model to clarify the nutritional regulation of SI-HDL. HDL in lymph perfusates collected under different nutritional conditions was analyzed by non-SDS-PAGE followed by Western blot analysis for apo AI. As shown in **Fig. 7A**, plasma HDL-C levels and the contents of HDL-apo AI in SI lymph perfusates from WT mice ad libitum were markedly reduced after 24 h fasting. In contrast, a 4-week high-fat diet markedly increased plasma HDL-C levels and the contents of HDL-apo AI in lymph perfusates from WT mice (Fig. 7B). These results indicate that fasting reduces and high-fat diet increases the production of HDL from the SI.

Apo E KO reduces the production of HDL from the SI

Apo E KO mice are characterized by a marked reduction of HDL-C levels in plasma. Because intestinal HDL has been shown to significantly contribute to plasma HDL (16), we used our in situ perfusion model to examine whether

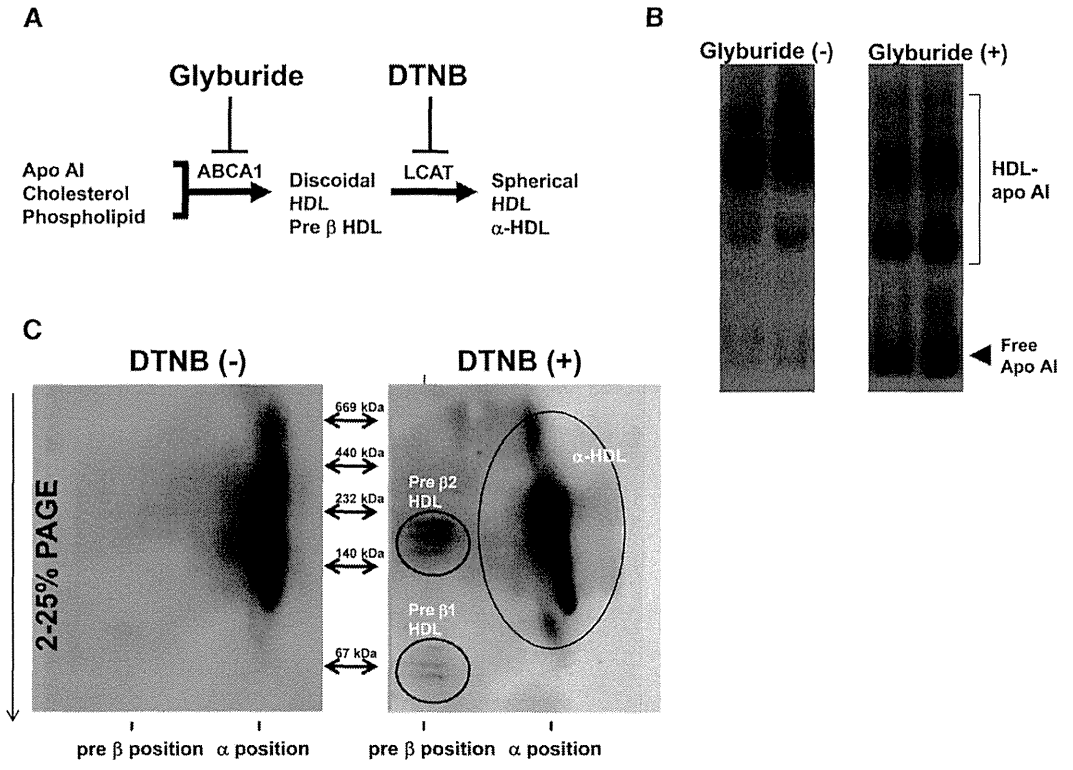

Fig. 6. Effects of glyburide and DTNB on the assembly of SI-HDL. A: Possible mechanism for the assembly of SI-HDL. Glyburide and DTNB are known inhibitors of ABCA1 and LCAT, respectively. B: Effect of glyburide on immunoblot patterns of HDL in SI lymph perfusates from WT mice. WT mice were subjected to in situ SI perfusion in the presence (right panel) and absence (left panel) of glyburide in the perfusion buffer. SI-HDL was run on non-SDS-PAGE followed by the detection of apo AI. Arrowhead represents free apo AI. C: Effect of DTNB on the formation of SI-HDL. SI lymph perfusates were obtained from WT mice that were perfused using a perfusion buffer in the presence (right panel) and absence (left panel) of DTNB in the perfusion buffer.

the production of HDL from the SI is reduced in apo E KO mice. As shown in Fig. 7C, apo E KO mice had markedly lower levels of HDL-C and reduced contents of HDL-apo AI in SI lymph perfusates as compared with WT mice. These results indicate that apo E may play a role in the biogenesis of SI-HDL.

DISCUSSION

To selectively evaluate HDL produced from the intestine, we developed an in situ perfusion model using surgically isolated mouse SI. Using our in situ perfusion model, we found that the SI produces HDL in mice and ABCA1 plays an important role in the production of SI-HDL, that SI-HDL is different from HDL produced by the liver, and that SI-HDL may be regulated by nutritional and genetic factors.

Our in situ perfusion model using surgically isolated mouse SI was developed for the selective evaluation of SI-HDL because HDL in mesenteric lymph collected from anesthetized mice originates either from the secretion by the SI or from the filtration from plasma through the blood capillary-lymph loop into the intestinal lymph duct (19–22).

Our novel in situ perfusion model achieves the selective evaluation of HDL by dissociating HDL production by the SI from the filtration of HDL from plasma. In this model, arterial blood supply for the SI is blocked by ligation of abdominal aorta and other arteries, leaving only the superior mesenteric artery open as the perfusion inlet (Fig. 1A). Perfusion buffer is pumped through a needle that is connected to a tube and inserted antegrade through the thoracic descending aorta into the abdominal aorta just before ligation of the abdominal aorta (Fig. 1A). Therefore, after perfusion starts, no additional systemic blood will enter the SI, and the possible filtration of plasma HDL from the systemic circulation into the SI lymph duct can be prevented. The SI lymph duct and portal vein are cannulated as outlets for perfusion buffer (Fig. 1A). Under these conditions, the HDL in the infusates collected from the SI lymph duct would originate only from the SI.

Using our in situ perfusion model, we found that HDL was detected in SI lymph perfusates from WT mice (Fig. 1B), indicating that the SI produces HDL. This finding supports the notion that the intestine, along with the liver, is an important site for the secretion of apo AI and the production of HDL (12–16). We did not detect HDL in SI lymph perfusates from ABCA1 mice (Fig. 1B), indicating that ABCA1 is essential for the production of HDL by the

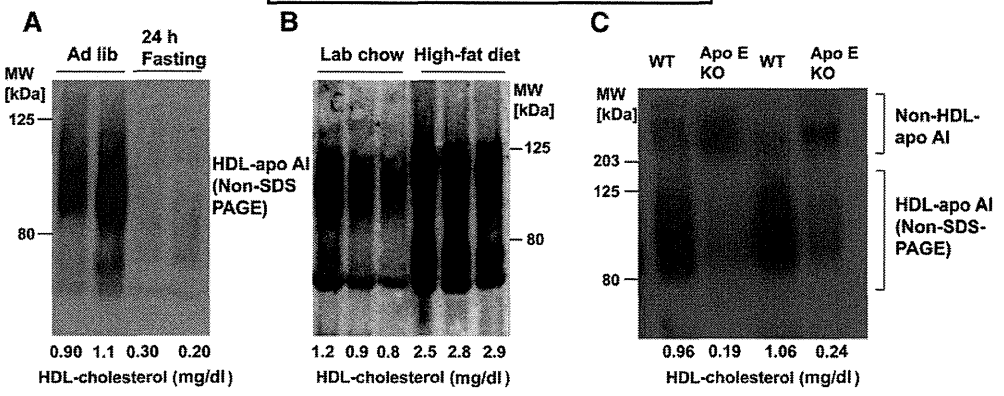

Fig. 7. Nutritional and genetic regulation of SI-HDL. The HDL-C concentration (mg/dl) in different perfusates was measured by HPLC as described in the Methods and is shown under each column. A: Effect of fasting on SI-HDL in WT mice. Mice were subjected to in situ perfusion at ad libitum and after 24 h of fasting. SI lymph perfusates were analyzed by using non-SDS-PAGE followed by Western blot analysis for apo AI. B: Effect of a high-fat diet on SI-HDL in WT mice. Mice were subjected to in situ SI perfusion after being fed a high-fat diet for 4 weeks. C: Comparison of SI-HDL production in 14-week-old WT and apo E KO mice.

SI. This finding supports those of Brunham et al. (16) that mice that specifically lack ABCA1 in the intestine had ~30% lower plasma HDL-C levels. However, we detected free apo AI in SI lymph perfusates from ABCA1 mice (Fig. 1B), indicating that cellular lipids are not available for the lipidation of apo AI to form SI-HDL in the absence of ABCA1 (45).

Because SI-HDL is not formed in the absence of ABCA1, we used ABCA1 KO mice to clarify whether plasma HDL can filtrate from the abdominal aorta through the SI into a lymph duct. We perfused the SI of ABCA1 KO mice using perfusion buffer to which had been added serum from WT mice and found that the collected SI lymph perfusates contained a substantial amount of HDL (Fig. 1C). It is possible that lipids in lipoproteins in the aortic perfusate may be delivered to the SI through transintestinal transport, that is, via the transintestinal cholesterol efflux pathway (48), and lipidate apo AI from intestinal secretion to form HDL. However, in the absence of ABCA1, which is located at the basolateral membrane of enterocytes (49), cellular lipids will not be available to free apo AI to form HDL. Therefore, HDL that was detected in SI lymph perfusates of ABCA1 mice perfused with serum from WT mice (Fig. 1C) can originate only from filtration of plasma HDL. Using our in situ perfusion model, we provided direct evidence that systemic plasma HDL can filtrate into the SI lymph duct.

One of the most likely mechanisms responsible for this perfusion is the "blood capillary-lymph loop" (50). Our finding that no apo B was present in SI lymph perfusates from ABCA1 KO mice that were perfused with buffer containing serum from WT mice indicated that HDL from the systemic circulation can, whereas apo-B-containing lipoproteins cannot, filter into the SI lymph duct (Fig. 1C), suggesting that bigger molecules cannot pass through the blood-capillary wall. Consistent with this finding, apo B48, but not apo B100, was detected in our analyses of apos in ultracentrifugation density fractions of lipoproteins in SI lymph perfusates from WT mice (Fig. 3B). Therefore, we consider the conventional cannulation experiment to be useful for the analysis of apo-B-containing lipoproteins because we used it to demonstrate an increase in the production of CMs in CD36 KO mice (51). However, for the selective evaluation of SI-HDL, the newly developed perfusion technique may be the best method available for eliminating the interference of plasma HDL.

Our finding that HDL was produced by the SI (Fig. 1A) but plasma HDL can also filtrate into the SI lymph duct (Fig. 1B) resolves controversies regarding intestinal-derived HDL (19–22). A previous study showed that HDL from the intestinal lymph duct obtained in vivo from anesthetized mice is likely to contain HDL from the systemic circulation, the majority of which is derived from the liver (16). Therefore, peptide mapping of HDL using LC/MS was performed to compare SI-HDL in SI lymph perfusates collected using our in situ perfusion model, C-HDL collected from the SI lymph duct in anesthetized mice, and L-HDL collected from liver perfusates (Fig. 2). C-HDL and L-HDL were very similar in that they had the same number of major peptides and relative peptide-ion intensities (Fig. 2C, D). This result agrees with the finding of Brunham et al. (16) that intestinal HDL in mice that lacked intestinal ABCA1 predominantly originates from the liver.

However, we found that SI-HDL in SI lymph perfusates was different from C-HDL and L-HDL in that SI-HDL contained additional major peptides (m/z 542 and m/z 524) that were not detected in L-HDL or C-HDL (Fig. 2). It is possible that the SI may secrete some known or unknown apos that are not secreted by the liver, and this proposition will need to be examined in future studies.

Our result that the two peptides (m/z 542 and m/z 524), which were detected as major peaks in SI-HDL obtained using our in situ perfusion model, were not detected in C-HDL obtained from the SI lymph duct in anesthetized mice (Fig. 2), suggests that rate of the production of HDL by the SI is slow as compared with that of filtration of pre-existing liver-originated HDL from the abdominal aorta into the SI lymph duct, and thus liver-originated HDL is

predominant in the SI lymph duct in anesthetized mice. This finding explains the result of Brunham et al. (16) that lymph from mice that specifically lack ABCA1 in the liver had no detectable HDL-C.

Our finding, obtained with peptide mapping of HDL using LC/MS, that C-HDL was very similar to L-HDL but different from SI-HDL (Fig. 2) further confirms our finding, obtained by perfusion of ABCA1 KO mice with serum from WT mice, that plasma HDL can filtrate from the abdominal aorta into the SI lymph duct (Fig. 1C). Therefore, our novel findings indicate that our in situ perfusion model can selectively evaluate HDL produced from the SI without possible interference from plasma HDL or HDL derived from the liver.

Using the novel in situ perfusion model, we characterized SI-HDL in comparison with plasma HDL and L-HDL. We found that SI-HDL had a much higher protein content and a lower lipid content than plasma HDL and that CE and PL were the major lipids (Table 1, Fig. 4A). Consistent with these findings, by examining SI-HDL using EM, we found that most SI-HDL was spherical and HDL was smaller than plasma HDL (Fig. 5). Our finding that SI-HDL is small and dense compared with plasma HDL suggests that SI-HDL may have higher antiatherogenic activity than plasma HDL (52).

When mice were fed ad libitum, SI-HDL separated from lymph perfusates by ultracentrifugation contained more TG and less CE than that from liver perfusates (Table 1), suggesting that the composition of core lipids of intestinal HDL is different from that of hepatic HDL. It is possible that HDL becomes TG rich due to fusion between nascent HDL and TG-rich lipoprotein (TRL). We have previously shown that HDL reconstituted from apo AI and PLs remodels plasma apo-B-containing lipoprotein from a patient with Tangier disease, which was TG rich (53), and from a patient with hypercholesterolemia (35). TG in HDL is known to be hydrolyzed by hepatic TG lipase. A lack of hepatic TG lipase in SI lymph perfusates may also lead to TG-rich SI-HDL.

Our analyses of apos in ultracentrifugation density fractions of lipoproteins in SI lymph perfusates showed that apo AIV and apo AI were distributed in both the HDL and non-HDL fractions (Fig. 3B). We compared the compositions of apos of intestinal and hepatic HDL in HDL density fractions separated from SI lymph perfusates and liver perfusates from WT mice using ultracentrifugation (Fig. 4B). We found that L-HDL contained a very limited amount of apo AIV but a considerable amount of apo E, whereas an opposite trend was seen with SI-HDL (Fig. 4B).

Ohta et al. (54) showed that apo AIV exists as a complex with apo AI. They separated apo-AIV-containing HDL using an anti-apo AIV immunoabsorbance column from a human lymph TRL fraction, lymph lipoprotein-deficient fraction (LDF), plasma HDL, and plasma LDF and analyzed apos after separation by SDS-PAGE. Also, Böttcher et al. (55), who separated plasma HDL into charge-based subfractions using preparative isotachophoresis, showed that slow-migrating HDL contained both apo AIV and apo AI, whereas fast-migrating HDL contained only apo AI. However, Duka et al. (56) showed that apo-AIV-containing HDL is formed in the absence of apo AI by using apo AI$^{-/-}$ mice that had been transfected with the apo AIV gene. Therefore, apo AIV coexists with apo AI but can form HDL independent of apo AI if apo AI is absent. It would be interesting to know whether apo-AIV-containing HDL is formed in patients with a genetic apo AI deficiency.

Apo AIV, which is mainly expressed in the SI, is a 46 kDa plasma protein associated with CM and HDL (54, 57) and reportedly can inhibit lipid oxidation and enhance cholesterol efflux. In addition, the overexpression of apo AIV was found to reduce atherosclerosis in mice models (58–60). Therefore, it would be of considerable interest to determine the function and relevance of SI-HDL, particularly with respect to atherosclerosis.

Because the examination of SI-HDL by EM showed spherical particles (Fig. 5), we examined the involvement of ABCA1 and LCAT in the formation of SI-HDL by using inhibitors of ABCA1 and LCAT (Fig. 6). We found that in SI lymph perfusates from WT mice markedly increased levels of free apo AI were detected in the presence of an ABCA1 inhibitor in the perfusion buffer, and pre-β-HDL appeared in the presence of an LCAT inhibitor in the perfusion buffer (Fig. 6). This finding indicates that both ABCA1 and LCAT may be involved in the formation of SI-HDL (2).

Complete inhibition of ABCA1 or LCAT was not achieved in our experiments, and this may have been due to technical reasons; that is, the selection and dosage of inhibitors was limited because of the sensitivity of the SI to the organic solvents (methanol and ethanol) used for solving the inhibitors. However, because we have shown that SI-HDL is rich in apo AIV, our finding is consistent with that of Duka et al. (56), who showed that ABCA1 and LCAT participate in the biogenesis of apo-AIV-containing particles by using ABCA1$^{-/-}$ and LCAT$^{-/-}$ mice that had been transfected with the apo AIV gene.

Using this novel in situ perfusion model, we also found that fasting drastically reduced, and high-fat feeding drastically increased, HDL-apo AI and HDL-C levels in SI lymph perfusates from WT mice (Fig. 7A, B). Our findings indicate that the production of SI-HDL can be dynamically regulated by nutritional factors. It would be interesting to determine whether the ratio of apo AI in HDL to lipid-poor apo AI is similar under different dietary conditions. Our in situ perfusion model should be useful for further investigating the regulation of the production of SI-HDL by various diet components such as saturated and unsaturated fatty acids.

We found that the production of SI-HDL was markedly reduced in the major experimental murine model for atherosclerosis, apo E KO mice (Fig. 7C). Reduced HDL-apo AI and HDL-C in SI lymph perfusates from apo E KO mice may be caused by a redistribution of apos from HDL to non-HDL due to substantial hyperlipidemia and abnormal lipoprotein metabolism. Our results showed that apo AI in SI lymph perfusates was distributed in HDL in WT mice but was distributed in non-HDL in apo E KO mice (Fig. 7C). Duka et al. (56) showed that apo AIV was contained

in HDL in apo $AI^{-/-}$ mice but was redistributed to non-HDL in apo $AI^{-/-}$ × apo $E^{-/-}$ mice.

Using our in situ perfusion model, we obtained novel information regarding the production of HDL by the SI, the characteristics of SI-HDL, and the regulation of HDL. However, this model is limited because the effects of anesthesia on gut motility and intestinal lipid trafficking are not clear.

The inhibition of cholesteryl ester transfer protein (CETP) may be a strategy for raising HDL. However, it has been demonstrated that such a strategy needs to be reconsidered because some clinical trials with CETP inhibitors have failed and been terminated (61–63). We reported in the 1990s that genetic human CETP deficiency was atherogenic rather than beneficial (64–66). Based on both these previous and current studies, an increase in the production of SI-HDL may be a therapeutic target for raising HDL.

In summary, we have shown that our in situ perfusion model using surgically isolated mouse SI achieves the selective evaluation of HDL produced from the intestine. Using this model, we showed that the production of HDL from the SI in mice requires ABCA1, and that SI-HDL is different from HDL produced by the liver and is regulated by nutritional and genetic factors. Because the intestine is a promising target for raising HDL, our in situ perfusion model represents a useful tool for developing novel strategies for the prevention and treatment of atherosclerosis. In addition, the SI performs various important functions in not only lipid homeostasis (67) but also immune defense as well as the production of hormones and cytokines. Therefore, our novel in situ perfusion system, which can be used in other spontaneous and genetically engineered mouse models, may also be a useful research tool for investigating physiological and pathological conditions in the SI and adjacent organs.

The authors thank Drs. Seiichiro Tarui and Masao Kawasaki for their helpful comments and discussion, Dr. Kazumitsu Ueda for providing antibody against ABCA1, and Mr. Jan K. Visscher for editing and proofreading the manuscript.

REFERENCES

1. Rader, D. J. 2006. Molecular regulation of HDL metabolism and function: implications for novel therapies. *J. Clin. Invest.* **116:** 3090–3100.
2. Nicholls, S. J., K. A. Rye, and P. J. Barter. 2005. High-density lipoproteins as therapeutic targets. *Curr. Opin. Lipidol.* **16:** 345–349.
3. Miller, N. E. 1990. Raising high density lipoprotein cholesterol. The biochemical pharmacology of reverse cholesterol transport. *Biochem. Pharmacol.* **40:** 403–410.
4. Miller, G. J., and N. E. Miller. 1975. Plasma-high-density-lipoprotein concentration and development of ischaemic heart-disease. *Lancet.* **1:** 16–19.
5. Castelli, W. P., J. T. Doyle, T. Gordon, C. G. Hames, M. C. Hjortland, S. B. Hulley, A. Kagan, and W. J. Zukel. 1977. HDL cholesterol and other lipids in coronary heart disease. The cooperative lipoprotein phenotyping study. *Circulation.* **55:** 767–772.
6. Brooks-Wilson, A., M. Marcil, S. M. Clee, L. H. Zhang, K. Roomp, M. van Dam, L. Yu, C. Brewer, J. A. Collins, H. O. Molhuizen, et al. 1999. Mutations in ABC1 in Tangier disease and familial high-density lipoprotein deficiency. *Nat. Genet.* **22:** 336–345.
7. Bodzioch, M., E. Orso, J. Klucken, T. Langmann, A. Bottcher, W. Diederich, W. Drobnik, S. Barlage, C. Buchler, M. Porsch-Ozcurumez, et al. 1999. The gene encoding ATP-binding cassette transporter 1 is mutated in Tangier disease. *Nat. Genet.* **22:** 347–351.
8. Rust, S., M. Rosier, H. Funke, J. Real, Z. Amoura, J. C. Piette, J. F. Deleuze, H. B. Brewer, N. Duverger, P. Denefle, et al. 1999. Tangier disease is caused by mutations in the gene encoding ATP-binding cassette transporter 1. *Nat. Genet.* **22:** 352–355.
9. Murthy, S., E. Born, S. N. Mathur, and F. J. Field. 2002. LXR/RXR activation enhances basolateral efflux of cholesterol in CaCo-2 cells. *J. Lipid Res.* **43:** 1054–1064.
10. Ohama, T., K. Hirano, Z. Zhang, R. Aoki, K. Tsujii, Y. Nakagawa-Toyama, K. Tsukamoto, C. Ikegami, A. Matsuyama, M. Ishigami, et al. 2002. Dominant expression of ATP-binding cassette transporter-1 on basolateral surface of Caco-2 cells stimulated by LXR/RXR ligands. *Biochem. Biophys. Res. Commun.* **296:** 625–630.
11. Iqbal, J., K. Anwar, and M. M. Hussain. 2003. Multiple, independently regulated pathways of cholesterol transport across the intestinal epithelial cells. *J. Biol. Chem.* **278:** 31610–31620.
12. Johansson, C., S. Rossner, and G. Walldius. 1978. H.D.L. secretion from human intestinal tract. *Lancet.* **1:** 324–325.
13. Green, P. H., R. M. Glickman, C. D. Saudek, C. B. Blum, and A. R. Tall. 1979. Human intestinal lipoproteins. Studies in chyluric subjects. *J. Clin. Invest.* **64:** 233–242.
14. Green, P. H., A. R. Tall, and R. M. Glickman. 1978. Rat intestine secretes discoid high density lipoprotein. *J. Clin. Invest.* **61:** 528–534.
15. Timmins, J. M., J. Y. Lee, E. Boudyguina, K. D. Kluckman, L. R. Brunham, A. Mulya, A. K. Gebre, J. M. Coutinho, P. L. Colvin, T. L. Smith, et al. 2005. Targeted inactivation of hepatic Abca1 causes profound hypoalphalipoproteinemia and kidney hypercatabolism of apoA-I. *J. Clin. Invest.* **115:** 1333–1342.
16. Brunham, L. R., J. K. Kruit, J. Iqbal, C. Fievet, J. M. Timmins, T. D. Pape, B. A. Coburn, N. Bissada, B. Staels, A. K. Groen, et al. 2006. Intestinal ABCA1 directly contributes to HDL biogenesis in vivo. *J. Clin. Invest.* **116:** 1052–1062.
17. Joyce, C. W., E. M. Wagner, F. Basso, M. J. Amar, L. A. Freeman, R. D. Shamburek, C. L. Knapper, J. Syed, J. Wu, B. L. Vaisman, et al. 2006. ABCA1 overexpression in the liver of LDLr-KO mice leads to accumulation of pro-atherogenic lipoproteins and enhanced atherosclerosis. *J. Biol. Chem.* **281:** 33053–33065.
18. Lo Sasso, G., S. Murzilli, L. Salvatore, I. D'Errico, M. Petruzzelli, P. Conca, Z. Y. Jiang, L. Calabresi, P. Parini, and A. Moschetta. 2010. Intestinal specific LXR activation stimulates reverse cholesterol transport and protects from atherosclerosis. *Cell Metab.* **12:** 187–193.
19. Forester, G. P., A. R. Tall, C. L. Bisgaier, and R. M. Glickman. 1983. Rat intestine secretes spherical high density lipoproteins. *J. Biol. Chem.* **258:** 5938–5943.
20. Bearnot, H. R., R. M. Glickman, L. Weinberg, P. H. Green, and A. R. Tall. 1982. Effect of biliary diversion on rat mesenteric lymph apolipoprotein-I and high density lipoprotein. *J. Clin. Invest.* **69:** 210–217.
21. Sipahi, A. M., H. C. Oliveira, K. S. Vasconcelos, L. N. Castilho, A. Bettarello, and E. C. Quintao. 1989. Contribution of plasma protein and lipoproteins to intestinal lymph: comparison of long-chain with medium-chain triglyceride duodenal infusion. *Lymphology.* **22:** 13–19.
22. Vasconcelos, K. S., A. M. Sipahi, H. C. Oliveira, L. N. Castilho, N. De Luccia, and E. C. Quintao. 1989. Origin of intestinal lymph cholesterol in rats: contribution from luminal absorption, mucosal synthesis and filtration from plasma. *Lymphology.* **22:** 4–12.
23. Nutescu, E. A., N. L. Shapiro, and A. Chevalier. 2008. New anticoagulant agents: direct thrombin inhibitors. *Cardiol. Clin.* **26:** 169–187.
24. Kavin, H., N. W. Levin, and M. M. Stanley. 1967. Isolated perfused rat small bowel–technic, studies of viability, glucose absorption. *J. Appl. Physiol.* **22:** 604–611.
25. Windmueller, H. G., and A. E. Spaeth. 1972. Fat transport and lymph and plasma lipoprotein biosynthesis by isolated intestine. *J. Lipid Res.* **13:** 92–105.
26. Wang, N., D. L. Silver, C. Thiele, and A. R. Tall. 2001. ATP-binding cassette transporter A1 (ABCA1) functions as a cholesterol efflux regulatory protein. *J. Biol. Chem.* **276:** 23742–23747.
27. Dory, L., C. H. Sloop, L. M. Boquet, R. L. Hamilton, and P. S. Roheim. 1983. Lecithin:cholesterol acyltransferase-mediated modification of discoidal peripheral lymph high density lipoproteins: possible mechanism of formation of cholesterol-induced high density lipoproteins (HDLc) in cholesterol-fed dogs. *Proc. Natl. Acad. Sci. USA.* **80:** 3489–3493.
28. Sugano, T., K. Suda, M. Shimada, and N. Oshino. 1978. Biochemical and ultrastructural evaluation of isolated rat liver systems perfused with a hemoglobin-free medium. *J. Biochem.* **83:** 995–1007.

29. Rappsilber, J., M. Mann, and Y. Ishihama. 2007. Protocol for micro-purification, enrichment, pre-fractionation and storage of peptides for proteomics using StageTips. *Nat. Protoc.* **2:** 1896–1906.
30. Sano, S., S. Tagami, Y. Hashimoto, K. Yoshizawa-Kumagaye, M. Tsunemi, M. Okochi, and T. Tomonaga. 2014. Absolute quantitation of low abundance plasma APL1beta peptides at sub-fmol/mL level by SRM/MRM without immunoaffinity enrichment. *J. Proteome Res.* **13:** 1012–1020.
31. Usui, S., Y. Hara, S. Hosaki, and M. Okazaki. 2002. A new on-line dual enzymatic method for simultaneous quantification of cholesterol and triglycerides in lipoproteins by HPLC. *J. Lipid Res.* **43:** 805–814.
32. Okazaki, M., S. Usui, M. Ishigami, N. Sakai, T. Nakamura, Y. Matsuzawa, and S. Yamashita. 2005. Identification of unique lipoprotein subclasses for visceral obesity by component analysis of cholesterol profile in high-performance liquid chromatography. *Arterioscler. Thromb. Vasc. Biol.* **25:** 578–584.
33. Toshima, G., Y. Iwama, F. Kimura, Y. Matsumoto, M. Miura, J. Takahashi, H. Yasuda, N. Arai, H. Mizutani, K. Hata, et al. 2013. LipoSEARCH®; analytical GP-HPLC method for lipoprotein profiling and its applications. *J Biol Macromol.* **13:** 21–32.
34. Furusyo, N., M. Ai, M. Okazaki, H. Ikezaki, T. Ihara, T. Hayashi, S. Hiramine, K. Ura, T. Kohzuma, E. J. Schaefer, et al. 2013. Serum cholesterol and triglyceride reference ranges of twenty lipoprotein subclasses for healthy Japanese men and women. *Atherosclerosis.* **231:** 238–245.
35. Zhang, B., Y. Uehara, S. Hida, S. Miura, D. L. Rainwater, M. Segawa, K. Kumagai, K. A. Rye, and K. Saku. 2007. Effects of reconstituted HDL on charge-based LDL subfractions as characterized by capillary isotachophoresis. *J. Lipid Res.* **48:** 1175–1189.
36. Zhang, B., E. Kawachi, A. Matsunaga, S. Imaizumi, K. Noda, Y. Uehara, S. Miura, K. Yoshinaga, M. Kuroki, and K. Saku. 2012. Reactivity of direct assays for low-density lipoprotein (LDL) cholesterol toward charge-modified LDL in hypercholesterolemia. *Circ. J.* **76:** 2241–2248.
37. Zhang, B., A. Matsunaga, D. L. Rainwater, S. Miura, K. Noda, H. Nishikawa, Y. Uehara, K. Shirai, M. Ogawa, and K. Saku. 2009. Effects of rosuvastatin on electronegative LDL as characterized by capillary isotachophoresis: the ROSARY Study. *J. Lipid Res.* **50:** 1832–1841.
38. Zhang, B., A. Böttcher, S. Imaizumi, K. Noda, G. Schmitz, and K. Saku. 2007. Relation between charge-based apolipoprotein B-containing lipoprotein subfractions and remnant-like particle cholesterol levels. *Atherosclerosis.* **191:** 153–161.
39. Saku, K., B. Zhang, and K. Noda, and Patrol Trial Investigators. 2011. Randomized head-to-head comparison of pitavastatin, atorvastatin, and rosuvastatin for safety and efficacy (quantity and quality of LDL): the PATROL trial. *Circ. J.* **75:** 1493–1505.
40. Mills, G. L., P. A. Lane, and P. K. Weech. 1984. A guidebook to lipoprotein technique. *In* Laboratory Techniques in Biochemistry and Molecular Biology. R. H. Burdon and P. H. van Knippenberg, editors. Elsevier, New York, NY. 18–78.
41. Miida, T., K. Inano, T. Yamaguchi, T. Tsuda, and M. Okada. 1997. LpA-I levels do not reflect pre beta1-HDL levels in human plasma. *Atherosclerosis.* **133:** 221–226.
42. Miida, T., T. Yamada, U. Seino, M. Ito, Y. Fueki, A. Takahashi, K. Kosuge, S. Soda, O. Hanyu, K. Obayashi, et al. 2006. Serum amyloid A (SAA)-induced remodeling of CSF-HDL. *Biochim. Biophys. Acta.* **1761:** 424–433.
43. SAS Institute Inc. 2009. SAS Online Doc 9.2. SAS Institute Inc., Cary, NC.
44. Brunham, L. R., J. K. Kruit, T. D. Pape, J. S. Parks, F. Kuipers, and M. R. Hayden. 2006. Tissue-specific induction of intestinal ABCA1 expression with a liver X receptor agonist raises plasma HDL cholesterol levels. *Circ. Res.* **99:** 672–674.
45. McNeish, J., R. J. Aiello, D. Guyot, T. Turi, C. Gabel, C. Aldinger, K. L. Hoppe, M. L. Roach, L. J. Royer, J. de Wet, et al. 2000. High density lipoprotein deficiency and foam cell accumulation in mice with targeted disruption of ATP-binding cassette transporter-1. *Proc. Natl. Acad. Sci. USA.* **97:** 4245–4250.
46. Hirano, K., S. G. Young, R. V. Farese, Jr., J. Ng, E. Sande, C. Warburton, L. M. Powell-Braxton, and N. O. Davidson. 1996. Targeted disruption of the mouse apobec-1 gene abolishes apolipoprotein B mRNA editing and eliminates apolipoprotein B48. *J. Biol. Chem.* **271:** 9887–9890.
47. Shen, B. W., A. M. Scanu, and F. J. Kezdy. 1977. Structure of human serum lipoproteins inferred from compositional analysis. *Proc. Natl. Acad. Sci. USA.* **74:** 837–841.
48. Temel, R. E., and J. M. Brown. 2012. Biliary and nonbiliary contributions to reverse cholesterol transport. *Curr. Opin. Lipidol.* **23:** 85–90.
49. Bonamassa, B., and A. Moschetta. 2013. Atherosclerosis: lessons from LXR and the intestine. *Trends Endocrinol. Metab.* **24:** 120–128.
50. Granger, D. N., J. D. Valleau, R. E. Parker, R. S. Lane, and A. E. Taylor. 1978. Effects of adenosine on intestinal hemodynamics, oxygen delivery, and capillary fluid exchange. *Am. J. Physiol.* **235:** H707–H719.
51. Masuda, D., K. Hirano, H. Oku, J. C. Sandoval, R. Kawase, M. Yuasa-Kawase, Y. Yamashita, M. Takada, K. Tsubakio-Yamamoto, Y. Tochino, et al. 2009. Chylomicron remnants are increased in the postprandial state in CD36 deficiency. *J. Lipid Res.* **50:** 999–1011.
52. Kontush, A., P. Therond, A. Zerrad, M. Couturier, A. Negre-Salvayre, J. A. de Souza, S. Chantepie, and M. J. Chapman. 2007. Preferential sphingosine-1-phosphate enrichment and sphingomyelin depletion are key features of small dense HDL3 particles: relevance to antiapoptotic and antioxidative activities. *Arterioscler. Thromb. Vasc. Biol.* **27:** 1843–1849.
53. Uehara, Y., Y. Tsuboi, B. Zhang, S. Miura, Y. Baba, M. A. Higuchi, T. Yamada, K. A. Rye, and K. Saku. 2008. POPC/apoA-I discs as a potent lipoprotein modulator in Tangier disease. *Atherosclerosis.* **197:** 283–289.
54. Ohta, T., N. H. Fidge, and P. J. Nestel. 1984. Characterization of apolipoprotein A-IV complexes and A-IV isoforms in human lymph and plasma lipoproteins. *J. Biol. Chem.* **259:** 14888–14893.
55. Böttcher, A., J. Schlosser, F. Kronenberg, H. Dieplinger, G. Knipping, K. J. Lackner, and G. Schmitz. 2000. Preparative free-solution isotachophoresis for separation of human plasma lipoproteins: apolipoprotein and lipid composition of HDL subfractions. *J. Lipid Res.* **41:** 905–915.
56. Duka, A., P. Fotakis, D. Georgiadou, A. Kateifides, K. Tzavlaki, L. von Eckardstein, E. Stratikos, D. Kardassis, and V. I. Zannis. 2013. ApoA-IV promotes the biogenesis of apoA-IV-containing HDL particles with the participation of ABCA1 and LCAT. *J. Lipid Res.* **54:** 107–115.
57. Bisgaier, C. L., O. P. Sachdev, L. Megna, and R. M. Glickman. 1985. Distribution of apolipoprotein A-IV in human plasma. *J. Lipid Res.* **26:** 11–25.
58. Duverger, N., N. Ghalim, G. Ailhaud, A. Steinmetz, J. C. Fruchart, and G. Castro. 1993. Characterization of apoA-IV-containing lipoprotein particles isolated from human plasma and interstitial fluid. *Arterioscler. Thromb.* **13:** 126–132.
59. Qin, X., D. K. Swertfeger, S. Zheng, D. Y. Hui, and P. Tso. 1998. Apolipoprotein AIV: a potent endogenous inhibitor of lipid oxidation. *Am. J. Physiol.* **274:** H1836–H1840.
60. Duverger, N., G. Tremp, J. M. Caillaud, F. Emmanuel, G. Castro, J. C. Fruchart, A. Steinmetz, and P. Denefle. 1996. Protection against atherogenesis in mice mediated by human apolipoprotein A-IV. *Science.* **273:** 966–968.
61. Nissen, S. E., J. C. Tardif, S. J. Nicholls, J. H. Revkin, C. L. Shear, W. T. Duggan, W. Ruzyllo, W. B. Bachinsky, G. P. Lasala, E. M. Tuzcu, et al. 2007. Effect of torcetrapib on the progression of coronary atherosclerosis. *N. Engl. J. Med.* **356:** 1304–1316. [Erratum. 2007. *N. Engl. J. Med.* 357: 835.]
62. Barter, P. J., M. Caulfield, M. Eriksson, S. M. Grundy, J. J. Kastelein, M. Komajda, J. Lopez-Sendon, L. Mosca, J. C. Tardif, D. D. Waters, et al. 2007. Effects of torcetrapib in patients at high risk for coronary events. *N. Engl. J. Med.* **357:** 2109–2122.
63. Schwartz, G. G., A. G. Olsson, M. Abt, C. M. Ballantyne, P. J. Barter, J. Brumm, B. R. Chaitman, I. M. Holme, D. Kallend, L. A. Leiter, et al. 2012. Effects of dalcetrapib in patients with a recent acute coronary syndrome. *N. Engl. J. Med.* **367:** 2089–2099.
64. Hirano, K., S. Yamashita, Y. Kuga, N. Sakai, S. Nozaki, S. Kihara, T. Arai, K. Yanagi, S. Takami, M. Menju, et al. 1995. Atherosclerotic disease in marked hyperalphalipoproteinemia. Combined reduction of cholesteryl ester transfer protein and hepatic triglyceride lipase. *Arterioscler. Thromb. Vasc. Biol.* **15:** 1849–1856.
65. Hirano, K., S. Yamashita, N. Nakajima, T. Arai, T. Maruyama, Y. Yoshida, M. Ishigami, N. Sakai, K. Kameda-Takemura, and Y. Matsuzawa. 1997. Genetic cholesteryl ester transfer protein deficiency is extremely frequent in the Omagari area of Japan. Marked hyperalphalipoproteinemia caused by CETP gene mutation is not associated with longevity. *Arterioscler. Thromb. Vasc. Biol.* **17:** 1053–1059.
66. Hirano, K., S. Yamashita, and Y. Matsuzawa. 2000. Pros and cons of inhibiting cholesteryl ester transfer protein. *Curr. Opin. Lipidol.* **11:** 589–596.
67. Abumrad, N. A., and N. O. Davidson. 2012. Role of the gut in lipid homeostasis. *Physiol. Rev.* **92:** 1061–1085.

Clinica Chimica Acta 430 (2014) 134–139

Contents lists available at ScienceDirect

Clinica Chimica Acta

journal homepage: www.elsevier.com/locate/clinchim

Mean postprandial triglyceride concentration is an independent risk factor for carotid atherosclerosis in patients with type 2 diabetes

Mayumi Idei [a], Satoshi Hirayama [a,*], Noriko Miyake [a], Mika Kon [a], Yuki Horiuchi [a], Tsuyoshi Ueno [a], Kazunori Miyake [a], Naotake Satoh [b], Hidenori Yoshii [c], Keiko Yamashiro [c], Tomio Onuma [c], Takashi Miida [a]

[a] Department of Clinical Laboratory Medicine, Juntendo University Graduate School of Medicine, Hongo 2-1-1, Bunkyo-ku, Tokyo 113-8421, Japan
[b] Department of Clinical Laboratory, Juntendo Tokyo Koto Geriatric Medical Center, Shinsuna 3-3-20, Koto-ku, Tokyo 136-0075, Japan
[c] Department of Internal Medicine, Diabetes and Endocrinology, Juntendo Tokyo Koto Geriatric Medical Center, Shinsuna 3-3-20, Koto-ku, Tokyo 136-0075, Japan

ARTICLE INFO

Article history:
Received 30 August 2013
Received in revised form 14 December 2013
Accepted 17 December 2013
Available online 27 December 2013

Keywords:
Postprandial hypertriglyceridemia
Diabetic dyslipidemia
Carotid atherosclerosis

ABSTRACT

Background: Postprandial hypertriglyceridemia is a risk factor for atherosclerotic disease. However, the postprandial triglyceride (PTG) concentration fluctuates markedly and is poorly reproducible. The aim of this study was to determine whether the mean PTG (mean-PTG) concentration is a risk factor for carotid atherosclerosis in patients with type 2 diabetes.
Methods: We measured the fasting and postprandial lipid concentrations, and the maximum intima-media thickness (max IMT) of carotid arteries by ultrasound in 115 diabetic patients. A carotid plaque was defined as max IMT of >1.0 mm. The mean-PTG concentration was calculated from several PTG concentrations measured on different days during a 1-year follow-up period.
Results: PTG concentrations showed marked intra-individual variability, and ranged from 0.29 to 6.03 mmol/l. Patients with carotid plaques had higher mean-PTG concentrations than those without carotid plaques (1.51 ± 0.57 vs. 1.29 ± 0.47 mmol/l, $p = 0.025$). Neither fasting triglycerides nor one-point PTG concentrations differed between the two groups. Multivariate stepwise logistic regression analysis revealed that the mean-PTG concentration was significantly associated with carotid plaques [OR 1.20 (95% CI, 1.05–1.37), $p = 0.009$], even after adjusting for traditional risk factors including HDL-cholesterol, LDL-cholesterol, age, hypertension, and duration of diabetes.
Conclusions: The mean-PTG concentration is an independent risk factor for carotid atherosclerosis in patients with type 2 diabetes.

1. Introduction

Accumulating evidence suggests that postprandial hypertriglyceridemia is an important risk factor for cardiovascular disease (CVD) in patients with type 2 diabetes. Recent epidemiological studies have shown that the postprandial triglyceride (PTG) concentration is more closely associated with CVD than is the fasting triglyceride (FTG) concentration, which is independent of traditional CVD risk factors [1–4]. Triglyceride-rich lipoproteins (TRLs) are composed of chylomicrons (CM), very low-density lipoproteins (VLDL), and their remnants. Remnant lipoproteins increase in the postprandial state and have greater atherogenicity than their precursors [5–8]. Because hypertriglyceridemia is a common feature in patients with type 2 diabetes, the PTG concentration is likely to be a better predictor of CVD than the FTG concentration in these patients.

Despite its potential usefulness as a diagnostic marker, no clinical guidelines provide a definitive cutoff value for the PTG concentration. The PTG concentration is poorly reproducible and is affected considerably by the meal content and fasting interval [2,9,10]. Most studies evaluated the PTG concentration only once (one-point PTG) or after oral loading with a high-fat diet, which has a much greater fat content than regular meals. Therefore, repeated measurements of PTG might yield a more reliable marker for postprandial dyslipidemia. The aim of this study was to elucidate whether the mean PTG (mean-PTG) concentration is an independent risk factor for carotid atherosclerosis in patients with type 2 diabetes. To assess carotid atherosclerosis, we used carotid ultrasonography because it is a noninvasive and quantitative method and because the extent of carotid atherosclerosis is positively correlated with an increased risk of CVD [11,12].

2. Methods

2.1. Recruitment of study subjects

A total of 177 patients with type 2 diabetes were recruited from those who underwent carotid ultrasonography at Juntendo Tokyo Koto Geriatric Medical Center between April 2007 and March 2009. Type 2 diabetes was defined by the criteria of the Japan Diabetes Society [13]. Patients who received hypoglycemic medications or insulin

* Corresponding author. Tel.: +81 3 3813 3111x3373; fax: +81 3 5684 1609.
E-mail address: sthiraya@juntendo.ac.jp (S. Hirayama).

0009-8981/$ – see front matter © 2013 Elsevier B.V. All rights reserved.
http://dx.doi.org/10.1016/j.cca.2013.12.022

therapy, and/or lipid-lowering medications including statins and fibrates, were eligible. We excluded patients with the following disorders: acute or chronic infections, cancer, liver cirrhosis, biliary tract disease, pancreatitis, chronic kidney disease, endocrine disease, and steroid-induced diabetes. Finally, data for 115 patients were collected and analyzed. The study protocol was approved by the Juntendo Tokyo Koto Geriatric Medical Center Research Ethics Committee.

2.2. Study protocol

In all patients, lipoprotein profiles were determined at 1- to 3-month intervals at the outpatient clinic. As a rule, blood samples were obtained 2 to 4 h after breakfast. However, fasting blood samples were obtained once during the 1-year follow-up period within 4 weeks before/after the ultrasound examination. Fasting and postprandial blood samples were taken on different days. In each patient, all PTG concentrations were used to calculate the mean-PTG concentration, while the PTG concentration measured nearest to the time of ultrasonography was defined as the one-point PTG concentration. The number of measurements of postprandial blood samples for each patient is shown in Supplementary Fig. 1. For subgroup analysis, we calculated the average and standard deviation (SD) of the mean-PTG of 115 patients. The patients were then classified into three groups: Low group [(< average mean-PTG minus 1SD); <0.88 mmol/l (77.5 mg/dl)], Middle group [(average mean-PTG minus 1SD) to (average mean-PTG plus 1SD); 0.88–1.95 mmol/l (77.5–172.5 mg/dl)], and High group [(≥ average mean-PTG plus 1SD); ≥1.95 mmol/l (172.5 mg/dl)].

Anthropometric data and medical history were collected from the medical records. Diabetic retinopathy, nephropathy, and neuropathy were categorized as microvascular complications, while coronary heart disease (CHD), cerebrovascular disease, and peripheral arterial disease were categorized as macrovascular complications. Smoking status was assessed by a questionnaire. Hypertension was defined as a systolic blood pressure of ≥140 mmHg and/or diastolic blood pressure of ≥90 mmHg, or current use of antihypertensive medications. Dyslipidemia was defined as an FTG of ≥1.69 mmol/l (150 mg/dl), HDL-C of <1.04 mmol/l (40 mg/dl), or LDL-C of ≥3.63 mmol/l (140 mg/dl) according to the guideline of the Japan Atherosclerosis Society [14], or current use of lipid-lowering medications.

All patients received diet therapy based on treatment guidelines for diabetes recommended by the Japan Diabetes Society, and underwent nutritional guidance by a registered dietician before the 1-year follow-up period. The content of diet therapy was as follows: a total energy was calculated by standard body weight

Table 1
Patients' characteristics and laboratory data according to mean-PTG level.

	Low	Middle	High	*p*-value
N	17	76	22	
Age (years)	67.0 ± 7.9	64.2 ± 9.6	60.5 ± 10.9	0.10
Men	7 (41)	43 (57)	10 (45)	0.42
BMI (kg/m^2)	23.7 ± 3.1	25.0 ± 3.7	24.6 ± 3.0	0.35
Waist circumference (cm)	86.3 ± 7.0	88.0 ± 9.9	87.3 ± 9.4	0.79
Hypertension	11 (65)	47 (62)	14 (64)	1.0
Systolic BP (mmHg)	133 ± 15	133 ± 13	131 ± 12	0.88
Diastolic BP (mmHg)	81 ± 10	79 ± 9	79 ± 9	0.67
Dyslipidemia	11 (65)	63 (83)	22 (100)**†	0.007
Duration of diabetes (years)	8.5 ± 7.3	9.7 ± 6.3	11.7 ± 7.0	0.30
Micro-/macrovascular complications	6 (35)/2 (12)	37 (49)/23 (30)	11 (50)/10 (45)	0.64/0.07
Current smoker[a]	5 (33)	27 (42)	12 (55)	0.44
Medications				
ACE inhibitors or ARBs	3 (18)	22 (29)	5 (23)	0.67
Calcium channel blockers	3 (18)	15 (20)	8 (36)	0.27
β-Blockers/diuretics	0 (0)/0 (0)	1 (1)/2 (3)	1 (5)/2 (9)	0.57
Statins/fibrates	4 (24)/1 (6)	22 (29)/3 (4)	10 (45)/1 (5)	0.27/0.82
Oral hypoglycemic agents/insulin	14 (82)/1 (6)	61 (80)/4 (5)	20 (91)/4 (18)	0.57/0.14
Fasting data				
FPG (mmol/l)	7.6 ± 2.2	7.7 ± 2.5	8.3 ± 2.7	0.60
A1C (%)	7.8 ± 1.7	7.4 ± 1.2	8.2 ± 2.0	0.31
Insulin (pmol/l)[b]	25 ± 13	49 ± 39**	68 ± 86**	<0.001
HOMA-IR[b]	1.2 ± 0.7	2.6 ± 3.0**	4.4 ± 7.7**	0.003
FTG (mmol/l)	0.75 ± 0.22	1.20 ± 0.37**	2.01 ± 0.54**‡	<0.001
TC (mmol/l)	4.86 ± 0.91	5.28 ± 0.85	5.66 ± 1.13*	0.028
HDL-C (mmol/l)	1.62 ± 0.31	1.35 ± 0.33**	1.22 ± 0.24**	<0.001
LDL-C (mmol/l)[c]	2.89 ± 0.80	3.39 ± 0.69	3.51 ± 1.05	0.07
ApoB (g/l)	0.82 ± 0.20	1.00 ± 0.18**	1.14 ± 0.25**†	<0.001
ApoCIII (g/l)	0.07 ± 0.02	0.09 ± 0.02	0.12 ± 0.03**‡	<0.001
ApoE (g/l)	0.04 ± 0.01	0.04 ± 0.01	0.05 ± 0.01*†	0.013
RLP-C (mmol/l)	0.08 ± 0.03	0.11 ± 0.04*	0.16 ± 0.07**‡	<0.001
FFA (mmol/l)	0.66 ± 0.20	0.49 ± 0.20**	0.54 ± 0.20	0.001
hs-CRP (mg/l)	0.27 (0.20–3.00)	0.71 (0.33–1.74)	1.31 (0.61–3.62)	0.05
Postprandial data				
One-point PTG (mmol/l)	0.77 ± 0.20	1.26 ± 0.47**	2.40 ± 0.87**‡	<0.001
Mean-PTG (mmol/l)	0.75 ± 0.12	1.31 ± 0.29**	2.27 ± 0.29**‡	<0.001

Data are expressed as *n* (%), mean ± SD, or median (interquartile).
The Low group was defined as a mean-PTG of <0.88 (mean − 1SD) mmol/l, the Middle group as a mean-PTG of 0.88–1.95 (mean ± 1 SD) mmol/l, and the High group as a mean-PTG of >1.95 (mean + 1SD) mmol/l.
BP, blood pressure; FPG, fasting plasma glucose; FTG, fasting triglyceride; PTG, postprandial triglyceride.
*$p < 0.05$, **$p < 0.01$ vs. Low; †$p < 0.05$, ‡$p < 0.01$ vs. Middle.
[a] Smoking status data were missing for 2 subjects in the Low group and for 11 subjects in the Middle group.
[b] We excluded 9 patients from the analysis (1 from the Low group, 4 from the Middle group, and 4 from the High group) because they were treated with insulin. HOMA-IR, as a marker of insulin resistance, was calculated using the formula: FPG (mg/dl) × fasting insulin (μU/ml) / 405.
[c] LDL-C was calculated by the Friedewald formula. In all samples, FTG concentrations were <4.52 mmol/l (400 mg/dl).

(=[height (m)]^2 × 22) (kg) × 25–30 kcal/kg, determined by the amount of individual physical activity. The ratio of protein, fat, and carbohydrate (PFC ratio) were 15%–20%, 20%–25%, and 50%–60%, respectively. Patients were instructed to take one third of the total calorie at breakfast and to not alter the PFC ratio for each meal. Consuming alcohol was avoided the day before the blood test.

2.3. Laboratory tests

Laboratory tests were performed on a Hitachi 7180 analyzer (Hitachi, Tokyo, Japan) unless otherwise indicated. Plasma glucose was measured enzymatically, while plasma insulin was measured by electrochemiluminescence immunoassay (ECLusys Insulin; Roche Diagnostics Japan, Tokyo) using a Cobas 6000 (Roche Diagnostic Japan). A1C was determined by high-performance liquid chromatography (HLC-723G7; Tosoh, Tokyo) and expressed as National Glycohemoglobin Standardization Program (NGSP) values [15]. Total cholesterol (TC), TG, and free fatty acid (FFA) were measured enzymatically (NEFA-SS; Eiken Chemical, Tokyo). LDL-C was calculated by the Friedewald formula [14] using overnight fasting samples. In all samples, FTG concentrations were <4.52 mmol/l (400 mg/dl). HDL-C was determined by a homogeneous method (Cholestest N HDL; Sekisui Medical, Tokyo). Remnant-like particle-cholesterol (RLP-C) was measured by an immunoseparation method (JIMRO II; Otsuka, Tokyo). Apolipoproteins were measured by an immunoturbidimetric method (B, CIII, E Auto N [Daiichi]; Sekisui Medical). High-sensitivity C-reactive protein (hs-CRP) was determined by a latex-enhanced immunonephelometric method (Bering Nepherometer II; Siemens Healthcare Diagnostics, Tokyo).

2.4. Assessment of carotid plaque

In the supine position, the bilateral walls of the common carotid arteries, carotid bulbs, and internal carotid arteries were visualized using a linear array 11-MHz transducer with a Philips SONOS 5500 (Philips Electronics Japan, Tokyo). The maximum intima-media thickness (max IMT) was measured in the observable areas. A carotid plaque was defined as max IMT of >1.0 mm with a point of inflection on the surface of the intima-media complex [16]. All ultrasound examinations were performed by two experienced laboratory technicians, and the recorded images were stored as digital data. The IMT was measured by one physician (M.I) using recorded images of the carotid artery. The personnel performing these procedures were blinded to the patient's clinical characteristics and laboratory test results.

2.5. Statistical analysis

Statistical analyses were performed using Stat Flex ver.6 for Windows (Artech Co., Ltd., Osaka, Japan). Results are expressed as number (%), mean ± SD, or median (interquartile). For categorical variables, 2- and 3-group comparisons were performed with the χ^2 test or Fisher's exact probability test. For continuous variables, 2-group comparisons were performed with Student's *t*-test or the Wilcoxon rank-sum test, while 3-group comparisons were performed with one-way ANOVA followed by Tukey test or Kruskal–Wallis test followed by Dunn test. Univariate and multivariate stepwise logistic regression analyses yielding odds ratios (ORs) and 95% confidence intervals (CIs) were used to identify risk factors for carotid plaques. A 2-tailed *p* value of <0.05 was considered statistically significance.

3. Results

3.1. Patients' characteristics and laboratory test results

The mean age was 63.9 ± 9.8 years, and the mean duration of diabetes was 9.9 ± 6.6 years in all subjects. Patients' characteristics and laboratory test results among the Low, Middle, and High groups classified by mean-PTG level are shown in Table 1. The prevalence of dyslipidemia was significantly higher in the High group than the Low and Middle groups. Other characteristics including age, hypertension, duration of diabetes, and proportion of current smokers did not differ among the groups. Although >60% of the patients had dyslipidemia in each of the three groups, most of them did not receive fibrates, and there was no significant difference in the number of patients who received fibrates among the groups. Insulin, HOMA-IR, FTG, apolipoproteins, and RLP-C were significantly higher, and HDL-C was significantly lower in the High group compared to the Low group. On the other hand, LDL-C did not differ among the three groups.

More than half of the study subjects had carotid plaques; thus, we compared the patient's background according to carotid plaques (Table 2). The plaque (+) group was 7.5 years older and had a 3.6-year longer duration of diabetes than the plaque (−) group. Furthermore, the prevalence of hypertension and macrovascular complications was 20% to 30% higher in the plaque (+) group than in the plaque (−) group. On the other hand, sex, BMI, waist circumference, and the proportion of current smokers were not significantly different between

Table 2
Patients' characteristics and laboratory data according to the presence or absence of carotid plaques.

	Plaque (−)	Plaque (+)	*p*-value
N	51	64	
Age (years)	59.7 ± 10.8	67.2 ± 7.4	<0.001
Men	22 (43)	38 (59)	0.08
BMI (kg/m^2)	24.9 ± 3.8	24.6 ± 3.3	0.70
Waist circumference (cm)	88.6 ± 10.3	86.9 ± 8.6	0.33
Hypertension	26 (51)	46 (72)	0.021
Systolic BP (mmHg)	132 ± 14	133 ± 12	0.89
Diastolic BP (mmHg)	81 ± 9	77 ± 9	0.032
Dyslipidemia	41 (80)	55 (86)	0.43
Duration of diabetes (years)	7.9 ± 5.3	11.5 ± 7.1	0.002
Micro-/macrovascular complications	19 (37)/6 (12)	35 (55)/29 (45)	0.06/<0.001
Current smoker[a]	16 (36)	28 (49)	0.17
Medications			
ACE inhibitors or ARBs	11 (22)	19 (30)	0.33
Calcium channel blockers	5 (10)	21 (33)	0.003
β-Blockers/diuretics	0 (0)/1 (2)	2 (3)/3 (5)	0.50/0.63
Statins/fibrates	15 (29)/3 (6)	21 (33)/2 (3)	0.70/0.65
Oral hypoglycemic agents/insulin	41 (80)/4 (8)	53 (83)/5 (8)	0.74/1.00
Fasting data			
FPG (mmol/l)	7.4 ± 2.2	8.2 ± 2.6	0.10
A1C (%)	7.5 ± 1.6	7.7 ± 1.4	0.35
Insulin (pmol/l)[b]	44 ± 30	52 ± 60	0.35
HOMA-IR[b]	2.2 ± 1.9	3.2 ± 5.2	0.17
FTG (mmol/l)	1.23 ± 0.44	1.34 ± 0.62	0.28
TC (mmol/l)	5.34 ± 0.86	5.26 ± 0.99	0.63
HDL-C (mmol/l)	1.45 ± 0.33	1.30 ± 0.32	0.019
LDL-C (mmol/l)[c]	3.33 ± 0.75	3.34 ± 0.85	0.94
ApoB (g/l)	0.99 ± 0.20	1.01 ± 0.23	0.57
ApoCIII (g/l)	0.09 ± 0.02	0.09 ± 0.03	0.55
ApoE (g/l)	0.04 ± 0.01	0.04 ± 0.01	0.48
RLP-C (mmol/l)	0.11 ± 0.04	0.12 ± 0.06	0.85
FFA (mmol/l)	0.53 ± 0.20	0.51 ± 0.21	0.79
hs-CRP (mg/l)	0.69 (0.25–1.77)	0.89 (0.32–2.15)	0.26
Postprandial data			
One-point PTG (mmol/l)	1.29 ± 0.60	1.49 ± 0.84	0.14
Mean-PTG (mmol/l)	1.29 ± 0.47	1.51 ± 0.57	0.025

Data are expressed as n (%), mean ± SD, or median (interquartile).
Abbreviations as in Table 1.
[a] Smoking status data were missing for 6 subjects in the plaque (−) group and for 7 subjects in the plaque (+) group.
[b] We excluded 9 patients from the analysis (4 from the plaque (−) group and 5 from the plaque (+) group) because they were treated with insulin. HOMA-IR was calculated as in Table 1.
[c] LDL-C was calculated as in Table 1.

the groups. Among many laboratory test results related to lipid and glucose metabolism, only HDL-C and mean-PTG showed a significant difference between the two groups. In the plaque (+) group, mean-PTG was higher and HDL-C was lower than in the plaque (−) group. It should be noted that neither FTG nor one-point PTG was significantly different between the groups.

3.2. Variability in PTG concentration

From the 115 patients, we took a total of 827 blood samples for PTG measurements (Fig. 1). The mean number of measurements was 7.2 ± 1.9 per patient (Supplementary Fig. 1). PTG concentration exhibit marked intra-individual variability, ranging from 0.29 to 1.32 mmol/l, 0.41 to 3.60 mmol/l, and 0.37 to 6.03 mmol/l in the Low, Middle, and High groups, respectively (Fig. 1). Even in the High group, 20% of the PTG values were <1.69 mmol/l. Individual coefficients of variation (CVs) of the PTG values ranged from 13.4% to 95.5% ($n = 115$, 31.6% ± 13.7%). There were no significant differences among the groups.

To determine the number of times that PTG measurement should be repeated to obtain stable mean-PTG values, we calculated the average PTG concentration at fewer sampling points (average PTG_x, where $x = 1, 2, 3...$) in each patient. The percentage difference between the mean-PTG and the average PTG_x [Δmean-PTG (%)] was obtained by the following equation: (average PTG_x − mean-PTG) × 100 / mean-PTG. The Δmean-PTG (%) steeply converged as the sampling number increased, and the 95% CI of the Δmean-PTG (%) of 5 measurements became approximately half as narrow as that of one measurement (95% CI: one measurement, −50% to 47%; 5 measurements, −25% to 16%) (Supplementary Fig. 2).

3.3. Relationship between mean-PTG concentration and carotid plaque

As the mean-PTG concentration increased, the prevalence of carotid plaques increased significantly. The χ^2 test revealed that the mean-PTG concentration had a significant effect on the incidence of carotid plaques (Fig. 2). The High group had a significantly higher prevalence of carotid plaques than did the Middle and Low groups. Univariate analysis also showed that the mean-PTG concentration was significantly associated with carotid plaques, as were other conventional risk factors such as age, hypertension, duration of diabetes, and HDL-C (Table 3). On the other hand, neither FTG nor one-point PTG had a significant association with carotid plaques.

Finally, we carried out multivariate stepwise logistic analysis with two models. A carotid plaque was used as the dependent variable in both models. Along with the other risk factors, either mean-PTG (Model A) or one-point PTG (Model B) was used as the independent variable. The mean-PTG, but not the one-point PTG, was selected as an independent risk factor for carotid plaques after adjustment for multiple risk factors including age, sex, BMI, hypertension, current smoker, A1C, HDL-C, and LDL-C [OR 1.20 (95% CI, 1.05–1.37), $p = 0.009$] (Table 4).

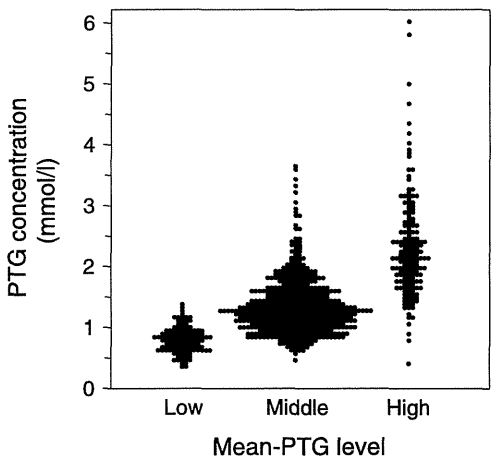

Fig. 1. Distribution of PTG concentration according to mean-PTG level. All PTG concentrations in each patient were plotted in the Low ($n = 17$, no. of samples = 120), Middle ($n = 76$, no. of samples = 535), and High ($n = 22$, no. of samples = 172) groups. The Low, Middle, and High groups were defined as in Table 1. PTG, postprandial triglycerides.

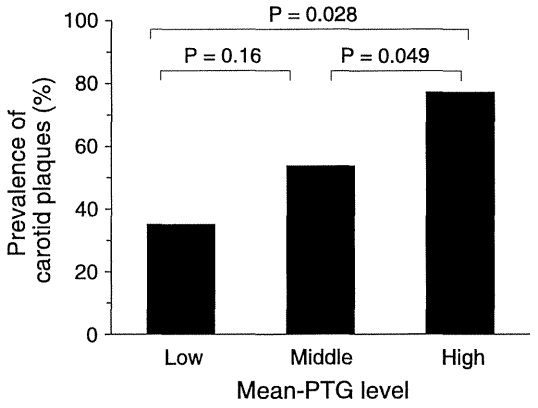

Fig. 2. Prevalence of carotid plaques according to mean-PTG level. The prevalence of carotid plaques was compared. The p value from χ^2 test among the 3 groups was 0.029. The results of χ^2 tests between each group are shown in the figure. The Low, Middle, and High groups were defined as in Table 1. PTG, postprandial triglycerides.

4. Discussion

Our results indicate that the mean-PTG concentration is an independent risk factor for carotid atherosclerosis and is superior to either the FTG or one-point PTG concentration in patients with type 2 diabetes. Multivariate stepwise logistic regression analysis revealed that the mean-PTG concentration, but not one-point PTG concentration, was associated with carotid atherosclerosis even after adjusting for other conventional risk factors such as HDL-C, LDL-C, age, hypertension, and duration of diabetes.

Dyslipidemia is common in patients with type 2 diabetes and is considered to promote atherosclerosis. Even in diabetic patients, LDL-C is a major risk factor for atherosclerotic disease. The lowering of LDL-C is the

Table 3
Univariate logistic regression analysis for carotid plaques.

Variable	Unadjusted OR (95% CI)	p-value
Age (years)	2.52 (1.56–4.08)	<0.001
Men	1.93 (0.91–4.06)	0.08
BMI (kg/m^2)	0.98 (0.88–1.09)	0.70
Hypertension	2.46 (1.13–5.33)	0.023
Current smoker	1.75 (0.79–3.90)	0.17
Duration of diabetes (years)	1.11 (1.03–1.19)	0.005
Fasting data		
A1C (%)	1.14 (0.87–1.47)	0.34
Insulin (pmol/l)	1.04 (0.95–1.14)	0.39
FTG (mmol/l)	1.04 (0.97–1.13)	0.29
HDL-C (mmol/l)	0.69 (0.51–0.95)	0.021
LDL-C (mmol/l)	1.01 (0.89–1.13)	0.94
ApoB (g/l)	1.05 (0.88–1.25)	0.58
ApoCIII (g/l)	1.05 (0.90–1.22)	0.56
ApoE (g/l)	0.88 (0.62–1.24)	0.46
RLP-C (mmol/l)	1.02 (0.81–1.28)	0.85
hs-CRP (mg/l)	1.06 (0.90–1.24)	0.48
Postprandial data		
One-point PTG (mmol/l)	1.04 (0.98–1.11)	0.16
Mean-PTG (mmol/l)	1.10 (1.01–1.19)	0.031

ORs are expressed for 10 unit increases in age and insulin, 0.11 unit (10 mg/dl) increases in TG, 0.26 unit (10 mg/dl) increases in HDL-C and LDL-C, 0.03 unit (1 mg/dl) increases in RLP-C, 0.1 unit increases in apoB, 0.01 unit increases in apoCIII and apoE, and 1 unit increases in other continuous variables. Abbreviations as in Table 1.

Table 4
Multivariate stepwise logistic regression analysis for carotid plaques, adjusted for conventional risk factors.

Variable	Adjusted OR (95% CI)	*p*-value
Model A[a]		
Age (years)	3.45 (1.80–6.61)	0.020
Hypertension	3.26 (1.15–9.62)	0.013
Duration of diabetes (years)	1.14 (1.04–1.26)	0.008
Mean-PTG (mmol/l)	1.20 (1.05–1.37)	0.009
Model B[b]		
Age (years)	2.74 (1.51–4.98)	<0.001
Hypertension	3.93 (1.22–12.7)	0.022
Duration of diabetes (years)	1.14 (1.04–1.25)	0.006

ORs are expressed for 10 unit increases in age, 1 unit increases in duration of diabetes, and 0.11 unit (10 mg/dl) increases in mean-PTG.
Models A and B were adjusted for age, sex, BMI, current smoker, hypertension, A1C, HDL-C, and LDL-C.
Abbreviations as in Table 1.
[a] Model A included age, sex, BMI, hypertension, current smoker, duration of diabetes, A1C, insulin, FTG, HDL-C, LDL-C, apoB, apoCIII, apoE, RLP-C, hs-CRP, and mean-PTG.
[b] Model B included all variables of Model A, except that mean-PTG was replaced by one-point PTG.

primary therapeutic target for diabetic dyslipidemia; this therapeutic goal is equivalent to that in patients with coronary artery disease. The guidelines of the American Diabetic Association recommend that the LDL-C concentration in patients with diabetes should be maintained at <2.59 mmol/l (100 mg/dl) [17]. However, many clinical trials have shown that statins, the most potent LDL-C-lowering drugs, reduce CVD events by only 25% to 50% [18,19].

High TG and low HDL-C concentrations are additional risk factors for macrovascular complications in patients with diabetes [20]. In a subanalysis of the Japan Diabetic Complication Study (JDCS), the TG concentration was the strongest predictor of CHD in Japanese females with diabetes [21]. Moreover, fibrates, which mainly reduce TG and raise HDL-C, significantly decreased CVD events in the patients with diabetes who had high TG concentrations [22,23]. Thus, both LDL-C and TG concentrations should be maintained within appropriate ranges.

Although PTG is more closely related to the development of atherosclerosis than is FTG [1–4], the marked intra-individual variability in the PTG concentration hinders the development of a consensus regarding the PTG concentration cutoff value [2,9,10]. Even in the High mean-PTG group in our study, the PTG concentration was within the normal range in 1 of every 5 blood samples (Fig. 1). To overcome these drawbacks of PTG, we adopted the mean values of several PTG concentrations measured at different times within 1 year. Our data suggest that the mean-PTG concentration calculated using more than five PTG values could be a stable marker of postprandial hypertriglyceridemia (Supplementary Fig. 2). The mean-PTG concentration can be calculated at any clinical institute and is readily applicable to daily medical practice.

The impact of the mean-PTG concentration on carotid atherosclerosis can be explained by the following mechanisms. In the postprandial state, CM is secreted from the intestine. Therefore, TRLs and their remnants accumulate in the circulation [5,6]. Remnants can enter the subendothelial space and be taken up without oxidation by macrophages. In diabetic patients with hypertriglyceridemia, TG-rich VLDL secretion is promoted in the liver due to high TG availability, while lipoprotein lipase (LPL) activity, a key enzyme for the catabolism of TRLs, is reduced. In the circulation, LPL hydrolyzes VLDL particles and forms LDL particles. Under the condition of abundant TRLs, cholesterol ester transfer protein (CETP) significantly transfers TG of TRLs to these LDL particles, which are hydrolyzed by hepatic lipase (HL). As a result, both LDL size and density further decrease, turning into atherogenic small dense LDLs (sd-LDLs), which are more atherogenic than large buoyant LDLs. Insulin resistance induces and exaggerates these abnormalities and promotes the formation of sd-LDLs [6,24–26]. In addition, high TRLs in the postprandial state may also contribute to proatherosclerotic and prothrombotic processes, including inflammation, oxidative stress, and endothelial dysfunction [20,24,25].

The mean-PTG concentration has some advantages over other markers related to TRLs, such as sd-LDL, apo CIII, and RLP-C. For example, the sd-LDL concentration is higher in patients with diabetes than in healthy subjects. As we reported previously, however, sd-LDL did not increase but rather decreased in the postprandial state [27]. Apo CIII resides mainly on TRLs and partly on HDL particles and inhibits LPL activity [28]. The apo CIII concentration is constant during the day [29]. Therefore, sd-LDL and apo CIII do not directly reflect postprandial hypertriglyceridemia. The RLP-C level could be another candidate marker of postprandial hyperlipidemia because it is elevated in the postprandial state [6,10,24,25]. Unfortunately, few studies have examined the association of postprandial RLP-C and atherosclerotic disease. On the other hand, several studies have demonstrated an association of the one-point PTG concentration or non-fasting TG concentration with CVD risk. Our results using the mean-PTG concentration are consistent with these observations [1–4,30].

In summary, the mean-PTG concentration is an independent risk factor for carotid atherosclerosis and is superior to either the FTG or one-point PTG concentration in patients with type 2 diabetes. Because the mean-PTG concentration is readily measured at outpatient clinics, the cutoff value should be determined in future studies.

Supplementary data to this article can be found online at http://dx.doi.org/10.1016/j.cca.2013.12.022.

Acknowledgements

The authors thank Munechika Segawa (Juntendo Tokyo Koto Geriatric Medical Center, Tokyo, Japan) for his technical assistance.

References

[1] Iso H, Naito Y, Sato S, et al. Serum triglycerides and risk of coronary heart disease among Japanese men and women. Am J Epidemiol 2001;153:490–9.
[2] Nordestgaard BG, Benn M, Schnohr P, et al. Nonfasting triglycerides and risk of myocardial infarction, ischemic heart disease, and death in men and women. JAMA 2007;298:299–308.
[3] Bansal S, Buring JE, Rifai N, et al. Fasting compared with nonfasting triglycerides and risk of cardiovascular events in women. JAMA 2007;298:309–16.
[4] Mora S, Rifai N, Buring JE, et al. Fasting compared with nonfasting lipids and apolipoproteins for predicting incident cardiovascular events. Circulation 2008;118:993–1001.
[5] Zilversmit DB. Atherogenesis: a postprandial phenomenon. Circulation 1979;60:473–85.
[6] Karpe F. Postprandial lipoprotein metabolism and atherosclerosis. J Intern Med 1999;246:341–55.
[7] McNamara JR, Shah PK, Nakajima K, et al. Remnant-like particle (RLP) cholesterol is an independent cardiovascular disease risk factor in women: results from the Framingham Heart Study. Atherosclerosis 2001;154:229–36.
[8] National Cholesterol Education Program (NCEP) Expert Panel on Detection, Evaluation, and Treatment of High Blood Cholesterol in Adults (Adult Treatment Panel III), Third Report of the National Cholesterol Education Program (NCEP) Expert Panel on Detection, Evaluation, and Treatment of High Blood Cholesterol in Adults (Adult Treatment Panel III) final report. Circulation 2002;106:3143–421.
[9] Cohn JS, McNamara JR, Cohn SD, et al. Plasma apolipoprotein changes in the triglyceride-rich lipoprotein fraction of human subjects fed a fat-rich meal. J Lipid Res 1988;29:925–36.
[10] Ai M, Tanaka A, Ogita K, et al. Relationship between plasma insulin concentration and plasma remnant lipoprotein response to an oral fat load in patients with type 2 diabetes. J Am Coll Cardiol 2001;38:1628–32.
[11] O'Leary DH, Polak JF, Kronmal RA, et al. Carotid-artery intima and media thickness as a risk factor for myocardial infarction and stroke in older adults. Cardiovascular Health Study Collaborative Research Group. N Engl J Med 1999;340:14–22.
[12] Jashari F, Ibrahimi P, Nicoll R, et al. Coronary and carotid atherosclerosis: similarities and differences. Atherosclerosis 2013;227:193–200.
[13] The Committee of the Japan Diabetes Society on the diagnostic criteria of diabetes mellitus. Report of the Committee on the classification and diagnostic criteria of diabetes mellitus. Diabetol Int 2010;1:2–20. http://dx.doi.org/10.1007/s13340-010-0006-7.
[14] Teramoto T, Sasaki J, Ueshima H, et al. Diagnostic criteria for dyslipidemia. Executive summary of Japan Atherosclerosis Society (JAS) guideline for diagnosis and prevention of atherosclerotic cardiovascular diseases for Japanese. J Atheroscler Thromb 2007;14:155–8.

[15] Kashiwagi A, Kasuga M, Araki E, et al. International clinical harmonization of glycated hemoglobin in Japan: from Japan Diabetes Society to National Glycohemoglobin Standardization Program values. Diabetol Int 2012;3:8–10. http://dx.doi.org/10.1007/s13340-012-0069-8.
[16] Terminology and Diagnostic Criteria Committee. Japan Society of Ultrasonics in Medicine. Standard method for ultrasound evaluation of carotid artery lesions. Jpn J Med Ultrasonics 2009;36:501–18. http://dx.doi.org/10.1007/s10396-009-0238-y.
[17] American Diabetes Association. Standards of medical care in diabetes-2013. Daibetes Care 2013;36(Suppl. 1):S11–66.
[18] Collins R, Armitage J, Parish S, et al. MRC/BHF Heart Protection Study of cholesterol-lowering with simvastatin in 5963 people with diabetes: a randomised placebo-controlled trial. Lancet 2003;361:2005–16.
[19] Colhoun HM, Betteridge DJ, Durrington PN, et al. Primary prevention of cardiovascular disease with atorvastatin in type 2 diabetes in the Collaborative Atorvastatin Diabetes Study (CARDS): multicentre randomised placebo-controlled trial. Lancet 2004;364:685–96.
[20] Mazzone T, Chait A, Plutzky J. Cardiovascular disease risk in type 2 diabetes mellitus: insights from mechanistic studies. Lancet 2008;371:1800–9.
[21] Sone H, Tanaka S, Tanaka S, et al. Comparison of various lipid variables as predictors of coronary heart disease in Japanese men and women with type 2 diabetes: subanalysis of the Japan Diabetes Complications Study. Diabetes Care 2012;35:1150–7.
[22] Keech A, Simes RJ, Barter P, et al. Effects of long-term fenofibrate therapy on cardiovascular events in 9795 people with type 2 diabetes mellitus (the FIELD study): randomised controlled trial. Lancet 2005;366:1849–61.
[23] ACCOD Study Group, Effects of combination lipid therapy in type 2 diabetes mellitus. N Engl J Med 2010;362:1563–74.
[24] Ginsberg HN, Illingworth DR. Postprandial dyslipidemia: an atherogenic disorder common in patients with diabetes mellitus. Am J Cardiol 2001;88:9H–15H.
[25] Taskinen MR. Diabetic dyslipidaemia: from basic research to clinical practice. Diabetologia 2003;46:733–49.
[26] Austin MA, Breslow JL, Hennekens CH, et al. Low-density lipoprotein subclass patterns and risk of myocardial infarction. JAMA 1988;260:1917–21.
[27] Hirayama S, Soda S, Ito Y, et al. Circadian change of serum concentration of small dense LDL-cholesterol in type 2 diabetic patients. Clin Chim Acta 2010;411:253–7.
[28] Bobik A. Apolipoprotein CIII and atherosclerosis: beyond effects on lipid metabolism. Circulation 2008;118:702–4.
[29] Kosuge K, Miida T, Takahashi A, et al. Estimating the fasting triglyceride concentration from the postprandial HDL-cholesterol and apolipoprotein CIII concentrations. Atherosclerosis 2006;184:413–9.
[30] Teno S, Uto Y, Nagashima H, et al. Association of postprandial hypertriglyceridemia and carotid intima-media thickness in patients with type 2 diabetes. Diabetes Care 2000;23:1401–6.

ACTA PÆDIATRICA
NURTURING THE CHILD

Acta Pædiatrica ISSN 0803-5253

REGULAR ARTICLE

Lipid profile and atherogenic indices soon after birth in Japanese preterm infants

Hiromichi Shoji (hshoji@juntendo.ac.jp)[1], Yayoi Murano[1], Mari Mori[1], Nobuaki Matsunaga[1], Natsuki Ohkawa[1], Hiroki Suganuma[1], Mitsuru Ikeno[1], Ken Hisata[1], Satoshi Hirayama[2], Tsuyoshi Ueno[2], Takashi Miida[2], Toshiaki Shimizu[1]

1.Department of Pediatrics, Juntendo University Faculty of Medicine, Tokyo, Japan
2.Department of Clinical Laboratory Medicine, Juntendo University Graduate School of Medicine, Tokyo Japan

Keywords
Apolipoproteins, Foetal growth restriction, Lipoproteins, Preterm infants

Correspondence
Hiromichi Shoji, M.D., Department of Pediatrics, Juntendo University Faculty of Medicine, 2-1-1 Hongo, Bunkyo-ku, Tokyo 113-8421, Japan.
Tel: +81-3-3813-3111 |
Fax: +81-3-5800-0216 |
E-mail: hshoji@juntendo.ac.jp

Received
3 May 2013; revised 19 August 2013; accepted 25 September 2013.

DOI:10.1111/apa.12436

ABSTRACT

Aim: The intra-uterine environment affects the risk of development of cardiovascular disease in adulthood. The aim of this study was to determine the influence of prematurity and foetal growth restriction on lipid metabolism, by assessing atherogenic indices soon after birth in preterm infants.

Methods: Blood samples were collected within 20 min of birth from 80 preterm infants with a gestational age of ≤35 weeks. Serum total cholesterol (TC), low-density lipoprotein cholesterol (LDLc), high-density lipoprotein cholesterol (HDLc), apolipoprotein-A1 (apoA1) and apolipoprotein-B (apoB) levels were measured. The ratio of TC/HDLc, LDLc/HDLc and apoB/apoA1 were also calculated. Correlations between these indices and gestational age, birth weight and the standard deviation (SD) score for birth weight were also determined.

Results: Gestational age, birth weight and SD score for birth weight were negatively correlated with the TC/HDLc, LDLc/HDLc and apoB/apoA1 ratios.

Conclusion: In preterm infants, prematurity and poor foetal growth may influence lipid and apolipoprotein metabolism and affect atherogenic indices at birth.

INTRODUCTION

Advances in neonatal intensive care in recent decades have brought about dramatic improvement in the prognosis for premature infants (1). However, as noted by Barker and Osmond in 1986 (2), evidence has accumulated that indices of foetal growth, such as size at birth, are inversely associated with cardiovascular morbidity and mortality (3–5). The intra-uterine environment and early postnatal life are now generally accepted as important determinants of the risk of cardiovascular disease in adulthood. Although the exact mechanisms are unknown, it has been suggested that abnormalities in the metabolism of serum lipids may explain these associations (6). Lipid metabolism is a subject of major importance in the nutrition of neonates because lipids are the main structural components of cell membranes and therefore affect growth and development. In a human study (7), low birth weight (BW) was found to be associated with higher total cholesterol (TC) concentrations in adult men. However, a recent systematic review of the literature on BW and blood cholesterol concluded that there was only a weak association between low BW and higher TC (8).

The lipoprotein profile in foetuses is quite different from that in adults because lipoprotein synthesis is low due to immature hepatic function and the absence of intestinal lipid absorption. The major plasma lipoprotein in foetuses is high-density lipoprotein (HDL), whereas in adults it is low-density lipoprotein (LDL) (9,10). Serum lipoprotein profiles in children are predictive of those in adulthood (11,12), and there is evidence that this association with adult levels may originate at birth (13,14). Several lipoprotein ratios or 'atherogenic indices' have been defined in an attempt to optimise the predictive capacity of the lipid profile. TC/HDL cholesterol (HDLc) and LDL cholesterol (LDLc)/HDLc ratios are risk indicators with a greater predictive value than isolated parameters used independently (15).

The major apoprotein present in HDL is apolipoprotein-A1 (apoA1), which provides structural stability to the spherical molecule. In LDL, apolipoprotein-B (apoB) constitutes most of the protein content. The apoB/apoA1 ratio is therefore also of great value in detecting atherogenic risk and is often more useful than TC/HDLc and LDLc/HDLc ratios (15).

Key notes

- The intra-uterine environment affects the risk of development of cardiovascular disease in adulthood.
- Blood samples were collected from 80 preterm infants within 20 min of birth to determine the influence of prematurity and foetal growth restriction on lipid metabolism.
- The results of this study show that based on measurements of lipids and apolipoproteins, prematurity and poor foetal growth may influence atherogenic indices.

Although there are many genetic and environmental factors besides BW that affect the foetal lipid and apolipoprotein profile in preterm infants, there is limited information linking the lipid and apolipoprotein profile to lipoprotein concentrations in later life. This study therefore measured lipids and apolipoprotein levels soon after birth in preterm infants, to assess the effect of prematurity and foetal growth on atherogenic indices.

MATERIALS AND METHODS

Study population

A pilot study was conducted in the neonatal intensive care unit (NICU) of Juntendo University Hospital, Tokyo, Japan. Singleton, preterm infants (gestational age, ≤35 weeks) who were born at our hospital between January 2010 and June 2012 were recruited to the study. Infants with major congenital abnormalities or metabolic disorders, as well as those born to women with diabetes mellitus, gestational diabetes, chronic hypertension, intra-uterine infections and the presence of fever (>37.8°C) or elevated c-reactive protein (≥2.0 mg/dL) prior to delivery, were excluded. Eleven of 91 eligible infants were excluded from the study, as six met one or more predefined exclusion criteria, and there were no lipid or apolipoproteins measurements for the other five. We studied a total of 80 (34 female and 46 male) preterm infants who were admitted during the study period. Gestational age (GA) was estimated from the mother's last menstrual period and confirmed through foetal ultrasound measurements. The mothers were between 28 and 44 years old, and none were vegetarians. Pregnancy-induced hypertension (PIH) was defined as a blood pressure >140/90 mmHg diagnosed after 20 weeks of gestation. Sex- and GA-independent SD score or percentiles for anthropometric parameters at birth were calculated by comparison with the Japanese standard birth weight curve (16). A small-for-gestational-age (SGA) infant was defined as a BW and birth height below the 10th percentile. This study was approved by the Institutional Review Board of Juntendo University Hospital, and prior written informed consent was obtained from parents of infants.

Biochemical measurements

The heel lance procedure was performed in the infants soon after admission to the NICU (within 20 min postpartum and before the first glucose infusion or first feeding). Blood samples (approximately 600 μL) were collected in heparin sodium-coated tubes. TC and triglyceride (TG) were measured enzymatically. LDLc and HDLc levels were measured directly by homogeneous assay, and apoA1 and apoB levels were determined by immune-turbidometric assay using a HITACHI Automatic Analyzer LABOSPECT008 (Hitachi High-Technologies Corporation, Tokyo, Japan).

Statistical analyses

Results are presented as the mean ± standard deviation (SD). Correlations between variables were evaluated using Spearman's rank correlation coefficient analysis. Values of $p < 0.05$ were considered to be statistically significant. All statistical analyses were performed using StatView 5.0 software (Abacus Concepts, Berkeley, CA, USA) and SPSS software for Windows version 11.0 (MapInfo Corporation, Troy, NY, USA).

RESULTS

Clinical characteristics and anthropometric indices of the mothers and infants included in this study are summarised in Table 1. Table 2 summarises the levels of TC, TG, HDLc, LDLc, apoA1 and apoB in preterm infants soon after birth. The mean GA and BW of the 80 infants were 31.7 weeks and 1450.5 g, respectively. Twenty-two (27.5%) SGA infants were included. The results of correlations between the lipids, apolipoproteins and the GA, BW and the SD score for BW are shown in Table 3. TG was negatively correlated with BW and SD score for BW ($p < 0.01$). LDLc and apoB were also negatively correlated with GA and BW ($p < 0.01$). HDLc was positively correlated with BW ($p < 0.05$) and SD score for BW ($p < 0.01$). The atherogenic indices of TC/HDLc, LDLc/HDLc and apoB/apoA1 were negatively correlated with GA, BW and SD score for BW (Fig. 1).

DISCUSSION

To our knowledge, this is the first study to assess atherogenic indices based on measurements of lipids and apolipoproteins in blood samples taken from preterm infants immediately postpartum. The results indicate that GA, BW and SD score for BW were negatively correlated with the atherogenic indices. This result was similar to the recent

Table 1 General subject characteristics. Data are presented as the mean ± SD or the number (percentage) of subjects

Mothers	
Age (years)	34.8 ± 4.4
Body weight before pregnancy(kg)	53.2 ± 8.9
BMI(kg/m^2)	20.2 ± 5.6
Body weight at delivery (kg)	61.6 ± 9.6
Antenatal steroids	26 (32.5%)
Infants	
Sex (M/F)	46/34
Gestational age (wks)	31.7 ± 3.1
<28 wks	12 (15.0%)
28–32 wks	31 (38.8%)
32 wks <	37 (46.3%)
Birth weight (g)	1450.5 ± 526.9
Body length (cm)	39.3 ± 5.3
SD score for birth weight	−1.1 ± 1.3
Head circumference (cm)	27.9 ± 3.6
Ponderal index(kg/m^3)	22.7 ± 2.1
Small for gestational age	22 (27.5%)
<28 wks/28–32 wks/32 wks<	6/8/8
5 min.- Apgar score <7	4 (5.0%)
Mechanical ventilation	28 (35.0%)